Chapter 4

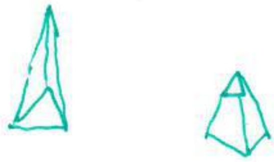

Earthquake Response of Structures

One of the most interesting and important applications of the study of structural dynamics is analyzing the response of structures subjected to ground motion caused by earthquakes.

Analytical solution of the equation of motion is not always possible when the applied force (or in the case of earthquake excitation, the ground motion) varies arbitrarily with time. Therefore, we must introduce numerical methods of evaluating the dynamic response.

4.1 Numerical Integration - can't represent w/ sine function

$m\ddot{u} + c\dot{u} + ku = -m\ddot{u}_g$

We have seen in the previous sections that the problem of analyzing MDOF systems with proportional damping becomes a problem of analyzing N SDOF systems, where N is the number of degrees of freedom and the size of the mass, stiffness, and damping matrix.

When the forcing function is described by a simple analytical function, then the solution for the problem can be derived first by using modal transformation to uncouple the equations of motion into the modal domain. The response for each mode is then calculated using the Duhamel's Integral. Finally, the response in the physical coordinates is found by transforming the modal response using $\boldsymbol{x} = \boldsymbol{\Phi y}$.

When the forcing function is no longer a simple analytical function, the terms involving Duhamel's integral may be quite cumbersome to calculate analytically. In order to solve this problem, we employ numerical integration to calculate Duhamel's integral.

The problem involves computing Duhamel's integral (Equation 2.224), which for a damped SDOF system subjected to an arbitrary force, $P(t)$, can be expressed as

$$x(t) = \frac{1}{m\omega_D}\int_0^t P(\tau)e^{-\zeta\omega_n(t-\tau)}\sin\omega_D(t-\tau)\,d\tau \tag{4.1}$$

Note: $\sin(u-v) = \sin u\cos v - \cos u \sin v$

Also $e^{-\zeta\omega_n(t-\tau)} = e^{-\zeta\omega_n t}e^{\zeta\omega_n\tau}$

The above equation can be rewritten as

$$x(t) = \frac{1}{m\omega_D}\int_0^t P(\tau)e^{-\zeta\omega_n(t-\tau)}(\sin\omega_D t\cos\omega_D\tau - \cos\omega_D t\sin\omega_D\tau)d\tau \tag{4.2}$$

which can be rearranged as

$$x(t) = Ae^{-\zeta\omega_n t}\sin\omega_D t - Be^{-\zeta\omega_n t}\cos\omega_D t \tag{4.3}$$

Potential mistake

where

corrects mistake

$$A = \frac{1}{m\omega_D}\int_0^t P(\tau)e^{+\zeta\omega_n\tau}\cos\omega_D\tau\, d\tau \tag{4.4a}$$

$$B = \frac{1}{m\omega_D}\int_0^t P(\tau)e^{+\zeta\omega_n\tau}\sin\omega_D\tau\, d\tau \tag{4.4b}$$

There are three simple ways to calculate the integrals described in Equations 4.4 numerically.

Rectangular rule The simplest method for numerical integration is by choosing an interpolation function that is a constant function over the time step. This is known as the *rectangular rule* or midpoint rule. For a function that passes directly through the point

$$(x, y) = \left[\frac{a+b}{2}, f\left(\frac{a+b}{2}\right)\right]$$

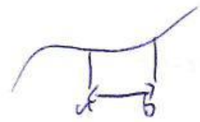

The definite integral can be approximated as

$$\int_a^b f(x)dx \approx (b-a)f\left(\frac{a+b}{2}\right) \tag{4.5}$$

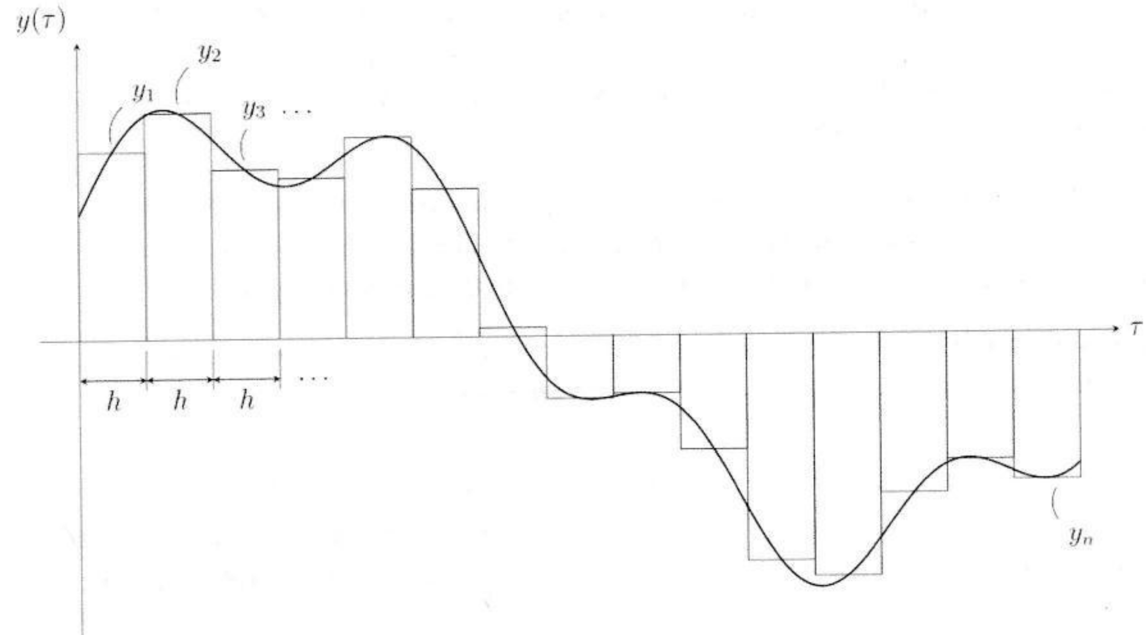

Figure 4.1 Numerical integration by rectangular rule

The integral of the function shown in Figure 4.1 from 0 to $\tau = t$ would be

$$\int_0^t y(\tau)d\tau \approx h\left(y_1 + y_2 + \dots + y_n\right) \tag{4.6}$$

Trapezoidal rule An improvement on the rectangular rule is using an interpolation function which passes through the points

$$(x_1, y_1) = [a, f(a)]$$
$$(x_2, y_2) = [b, f(b)]$$

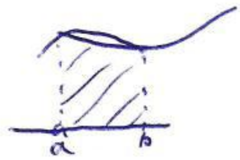

The definite integral can be approximated as

$$\int_a^b f(x)dx \approx (b-a)\left(\frac{f(a)+f(b)}{2}\right) \tag{4.7}$$

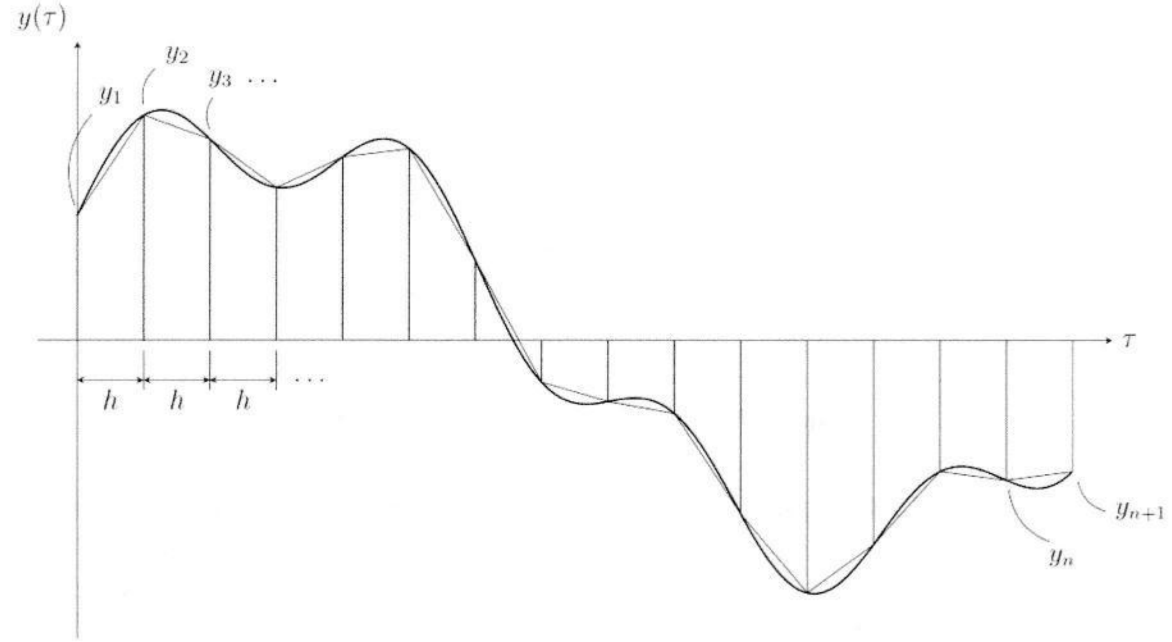

Figure 4.2 Numerical integration by trapezoidal rule

The integral of the function shown in Figure 4.2 from 0 to $\tau = t$ would be

$$\int_0^t y(\tau)d\tau \approx \frac{h}{2}\left(y_1 + 2y_2 + 2y_3 + \dots + 2y_n + y_{n+1}\right) \tag{4.8}$$

Simpson's rule The final method considered is Simpson's rule, which seeks to fit a quadratic polynomial function that takes the same values of $f(x)$ at the endpoints a and b, as well as the midpoint $a + b$. The integral can be approximated as follows:

3 points

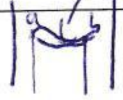

$$\int_a^b f(x)\,dx \approx \frac{b-a}{6}\left[f(a)+4f\left(\frac{a+b}{2}\right)+f(b)\right] \tag{4.9}$$

The integral of the function shown in Figure 4.2 from 0 to $\tau = t$ using Simpson's rule would be

$$\int_0^t y(\tau)\,d\tau = \frac{h}{3}\left(y_1+4y_2+2y_3+4y_4+\dots+4y_{n-1}+2y_n+y_{n+1}\right) \tag{4.10}$$

Example 4.1 Numerically evaluate the response to the half sine pulse shown in Figure 4.3 using the following system properties: $m = 2.53$ kip·s^2/in, $\omega_n = 6.283$ rad/s, and $\zeta = 0$.

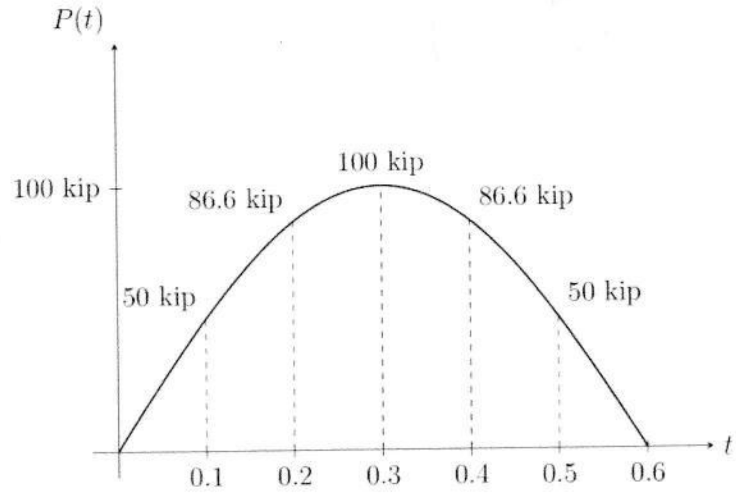

Figure 4.3 Half sine pulse forcing function

Solution: The MATLAB™ script used to perform numerical integration using the trapezoidal method is as follows:

```
dt=0.1; %s
d_tau=0.1;
m=2.53; % kip s^2/in
omega_n=6.283; % rad/s
zeta=0;
omega_D=omega_n*sqrt(1-zeta^2); % rad/s
A(1)=0;
B(1)=0;
t=0:dt:0.6;
tau=0:d_tau:0.6;
f_t=100*sin((2*pi/1.2)*tau); % kips
f_a=f_t.*exp(zeta*omega_n.*tau).*cos(omega_D.*tau);
```

$x(t) = Ae^{-\zeta\omega_n t}\sin\omega_D t - Be^{-\zeta\omega_n t}\cos\omega_D t$

```
f_b=f_t.*exp(zeta*omega_n.*tau).*sin(omega_D.*tau);
for i=2:length(f_t)
    A(i)=A(i-1)+1/2*dt*(f_a(i-1)+f_a(i));
    B(i)=B(i-1)+1/2*dt*(f_b(i-1)+f_b(i));
    y(i)=1/(m*omega_D)*(A(i)*exp(-zeta*omega_n*t(i))*sin(omega_D*t(i))-...
        B(i)*exp(-zeta*omega_n*t(i))*cos(omega_D*t(i)));
end
```

The numerical solution is compared to the analytical solution below.

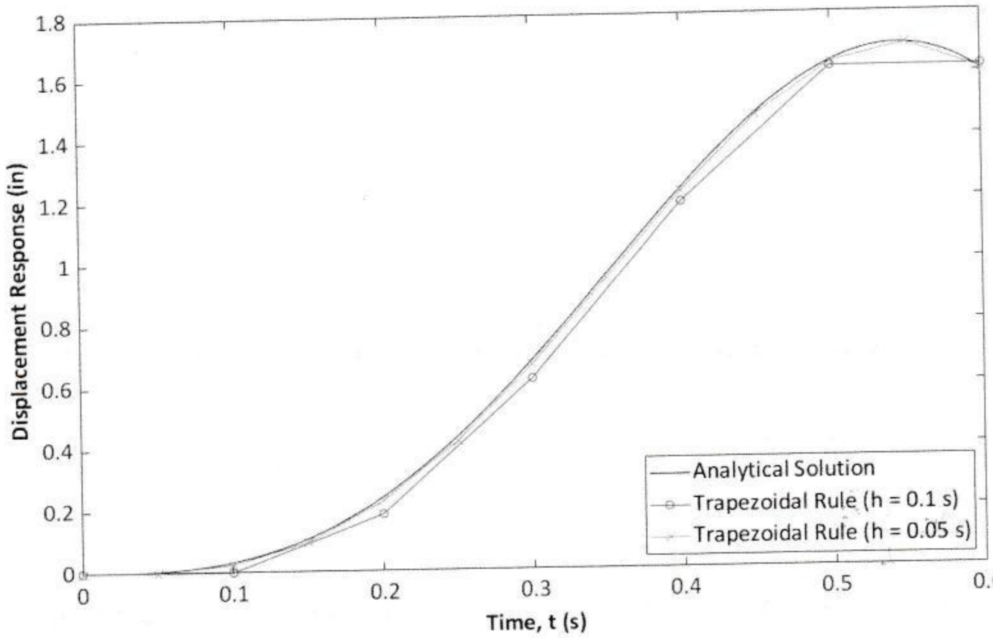

4.1.1 Newmark-β Method - looking at incremental Des in equilibrium !!

We will now investigate an alternative, more powerful method of solving the system of equations for arbitrary force excitations that are difficult to solve analytically. The method is known as the *Newmark-β method* and is used in some analysis software packages.

We will first consider linear system. We begin by deriving the equations of motion in an incremental form. At the i^{th} time instant, t_i

$$m\ddot{x}_i + c\dot{x}_i + kx_i = P_i \tag{4.11}$$

For the $(i+1)^{\text{th}}$ time instant, t_{i+1},

$$m\ddot{x}_{i+1} + c\dot{x}_{i+1} + kx_{i+1} = P_{i+1} \tag{4.12}$$

Subtracting Equation 4.11 from Equation 4.12 gives,

$$m\Delta\ddot{x}_i + c\Delta\dot{x}_i + k\Delta\dot{x} = \Delta P_i \tag{4.13}$$

where $\Delta\ddot{x}_i = \ddot{x}_{i+1} - \ddot{x}_i$, $\Delta\dot{x}_i = \dot{x}_{i+1} - \dot{x}_i$, $\Delta x_i = x_{i+1} - x_i$, and $\Delta P_i = P_{i+1} - P_i$.

The key to the Newmark-β method is how the change in acceleration is captured.

Average Acceleration The average acceleration model assumes the acceleration between the t_i and t_{i+1} is the average of the acceleration of the two instances.

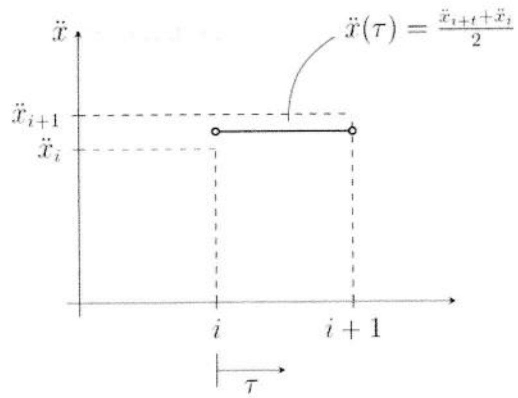

Figure 4.4 Average acceleration assumption in Newmark-β method

The acceleration is given by

$$\ddot{x}(\tau) = \frac{\ddot{x}_{i+1} + \ddot{x}_i}{2} \tag{4.14}$$

Integrating Equation 4.14, and solving for the constant using the boundary condition $\dot{x}(0) = \dot{x}_i$, we get

$$\dot{x}(\tau) = \dot{x}_i + \left(\frac{\ddot{x}_{i+1} + \ddot{x}_i}{2}\right)\tau \tag{4.15}$$

Integrating Equation 4.15, and applying the boundary condition $x(0) = x_i$, we get,

$$x(\tau) = x_i + \dot{x}_i\tau + \left(\frac{\ddot{x}_{i+1} + \ddot{x}_i}{2}\right)\frac{\tau^2}{2} \tag{4.16}$$

Hence, the velocity and displacement at t_{i+1} are (when $\tau = \Delta t$ in Equations 4.16 and 4.15)

$$\dot{x}_{i+1} = \dot{x}_i + \frac{\Delta t}{2}(\ddot{x}_{i+1} + \ddot{x}_i) \tag{4.17a}$$

$$x_{i+1} = x_i + \dot{x}_i\Delta t + \frac{(\Delta t)^2}{4}(\ddot{x}_{i+1} + \ddot{x}_i) \tag{4.17b}$$

Linear Acceleration The linear acceleration model assumes that the acceleration varies linearly between the i^{th} and the $(i+1)^{\text{th}}$ time step.

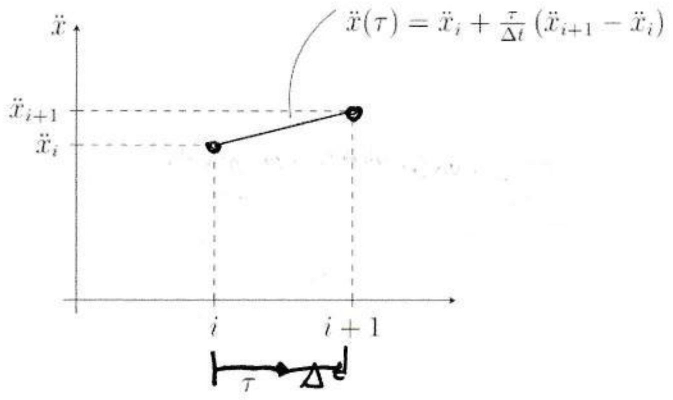

Figure 4.5 Linear acceleration assumption in Newmark-β method

The acceleration is given by

$$\ddot{x}(\tau) = \ddot{x}_i + \frac{\tau}{\Delta t}\left(\ddot{x}_{i+1} - \ddot{x}_i\right) \tag{4.18}$$

Integrating Equation 4.18, and solving for the constant using the boundary condition $\dot{x}(0) = \dot{x}_i$, we get

$$\dot{x}(\tau) = \dot{x}_i + \ddot{x}_i\tau + \left(\frac{\ddot{x}_{i+1} - \ddot{x}_i}{\Delta t}\right)\frac{\tau^2}{2} \tag{4.19}$$

Integrating Equation 4.19, and applying the boundary condition $x(0) = x_i$, we get,

$$x(\tau) = x_i + \dot{x}_i\tau + \ddot{x}_i\frac{\tau^2}{2} + \left(\frac{\ddot{x}_{i+1} - \ddot{x}_i}{\Delta t}\right)\frac{\tau^3}{6} \tag{4.20}$$

Hence, the velocity and displacement at t_{i+1} for the linear acceleration assumption are

Velocity
$$\dot{x}_{i+1} = \dot{x}_i + \ddot{x}_i\Delta t + \frac{\Delta t}{2}(\ddot{x}_{i+1} - \ddot{x}_i) \tag{4.21a}$$

Displacement
$$x_{i+1} = x_i + \dot{x}_i\Delta t + \ddot{x}_i\frac{(\Delta t)^2}{2} + \frac{(\Delta t)^2}{6}(\ddot{x}_{i+1} - \ddot{x}_i) \tag{4.21b}$$

The expressions for velocity and displacement can be generalized as

Similar to 4.17, except linear assumption

$$\dot{x}_{i+1} = \dot{x}_i + \left[(1-\gamma)\Delta t\right]\ddot{x}_i + (\gamma\Delta t)\ddot{x}_{i+1} \tag{4.22a}$$

$$x_{i+1} = x_i + \dot{x}_i\Delta t + \left[\left(\tfrac{1}{2}-\beta\right)(\Delta t)^2\right]\ddot{x}_i + \beta(\Delta t)^2\ddot{x}_{i+1} \tag{4.22b}$$

Setting $\gamma = 1/2$ and $\beta = 1/4$ yields Equations 4.17, the constant acceleration assumption. $\gamma = 1/2$ and $\beta = 1/6$ yields Equations 4.21, the linear acceleration assumption. The factors γ and β determine the stability and accuracy of the solution. In general,

$$\gamma = 1/2 \qquad (4.23a)$$

$$\frac{1}{6} \le \beta \le \frac{1}{4} \qquad (4.23b)$$

uncontrollable error growth

In any numerical method, stability and accuracy are important considerations. For the purposes of this course, we simply note that regardless of which approximation is used (constant average or linear), using small time steps, Δt, is necessary to ensure the response can be captured accurately. As a general rule, $\Delta t \le \min(T, T_n)/10$, where T and T_n are the excitation and natural periods respectively.

We can now use the approximations derived above to develop a solution to the incremental equation of motion given by Equation 4.13. Consider the general forms of velocity and displacement approximations. $m\Delta\ddot{x}_i + c\Delta\dot{x}_i + k\Delta x_i = \Delta P_i$

$$\dot{x}_{i+1} = \dot{x}_i + [(1-\gamma)\Delta t]\ddot{x}_i + (\gamma\Delta t)\ddot{x}_{i+1} \qquad (4.24a)$$

$$x_{i+1} = x_i + \dot{x}_i\Delta t + \left[\left(\frac{1}{2} - \beta\right)(\Delta t)^2\right]\ddot{x}_i + \beta(\Delta t)^2\ddot{x}_{i+1} \qquad (4.24b)$$

First, rearranging Equation 4.24a

$$\dot{x}_{i+1} - \dot{x}_i = [(1-\gamma)\Delta t]\ddot{x}_i + (\gamma\Delta t)\ddot{x}_{i+1}$$

$$\Delta\dot{x}_i = \Delta t\,\ddot{x}_i + (\gamma\Delta t)\Delta\ddot{x}_i \qquad (4.25)$$

Next, from Equation 4.24b,

$$x_{i+1} - x_i = \dot{x}_i\Delta t + \frac{(\Delta t)^2}{2}\ddot{x}_i - \beta(\Delta t)^2\ddot{u}_i + \beta(\Delta t)^2\ddot{x}_{i+1}$$

$$\Delta x_i = \dot{x}_i\Delta t + \frac{(\Delta t)^2}{2}\ddot{x}_i + \beta(\Delta t)^2(\ddot{x}_{i+1} - \ddot{x}_i) \qquad (4.27)$$

$$\Delta x_i = \dot{x}_i\Delta t + \frac{(\Delta t)^2}{2}\ddot{x}_i + \beta(\Delta t)^2\Delta\ddot{x}_i$$

Solving for $\Delta\ddot{x}_i$ in Equation 4.27 gives,

$$\Delta\ddot{x}_i = \frac{1}{\beta(\Delta t)^2}\Delta x_i - \frac{1}{\beta\Delta t}\dot{x}_i - \frac{1}{2\beta}\ddot{x}_i \qquad (4.28)$$

Substituting Equation 4.28 into Equation 4.25,

$$\Delta \dot{x}_i = \left(1-\frac{\gamma}{2\beta}\right)\Delta t\ddot{x}_i - \frac{\gamma}{\beta}\dot{x}_i + \frac{\gamma}{\beta\Delta t}\Delta x_i \tag{4.29}$$

Note that the change in acceleration and velocity from t_i to t_{i+1} given by Equation 4.28 and Equation 4.29 respectively, are dependent on the known acceleration and velocity at time i (i.e. $\ddot{x}_i$ and $\dot{x}_i$) and the change in displacement Δx_i. $m\Delta\ddot{x}_i + c\Delta\dot{x}_i + k\Delta x_i = \Delta P_i$

We can now substitute Equations 4.28 and 4.29 into the incremental equation of motion, Equation 4.13, and solve for the incremental displacement Δx_i.

Big Bad Equation

$$\left[k+\frac{1}{\beta(\Delta t)^2}m+\frac{\gamma}{\beta\Delta t}c\right]\Delta x_i = \Delta P_i + \left[\frac{1}{2\beta}m + \Delta t\left(\frac{\gamma}{2\beta}-1\right)c\right]\ddot{x}_i + \left(\frac{1}{\beta\Delta t}m+\frac{\gamma}{\beta}c\right)\dot{x}_i$$

$$\hat{k}\Delta x_i = \Delta\hat{P}_i \tag{4.30}$$

only unknown

$\hat{k}$ and $\Delta\hat{P}_i$ are only dependent on the system properties m, c, and k, the algorithm parameters γ, β, and the known state of the system at time i defined by x_i, $\dot{x}_i$, and $\ddot{x}_i$. Once the incremental displacement Δx_i is computed from Equation 4.30, the displacement at time $i+1$ is simply,

$$x_{i+1} = x_i + \Delta x_i \tag{4.31}$$

$\Delta\dot{x}_i$ and $\Delta\ddot{x}_i$ can be obtained from Equation 4.29 and 4.28, respectively, and the velocity and acceleration are updated in similar fashion

$$\dot{x}_{i+1} = \dot{x}_i + \Delta\dot{x}_i \tag{4.32}$$

$$\ddot{x}_{i+1} = \ddot{x}_i + \Delta\ddot{x}_i \tag{4.33}$$

After the response quantities have been computed at t_{i+1}, t_{i+1} becomes $t_i$as we move on to the next time step and start the process again. To initiate Newmark's method at $t=0$, we can compute the initial acceleration, $\ddot{x}_0$, from Equation 4.11 as

Specified

$$\ddot{x}_0 = \frac{P_0 - c\dot{x}_0 - kx_0}{m} \tag{4.34}$$

where x_0, $\dot{x}_0$, and P_0 are the displacement, velocity, and force initial conditions at $t=0$. Steps for analyzing linear SDOF systems using Newmark-β method is summarized below.

Newmark-β Method

Special cases:

- Constant average acceleration method ($\gamma = 1/2$, $\beta = 1/4$)
- Linear acceleration method ($\gamma = 1/2$, $\beta = 1/6$)

1.0 *Initial calculations*

1.1 $\ddot{x}_0 = \dfrac{P_0 - c\dot{x}_0 - kx_0}{m}$

1.2 Select Δt

1.3 $\hat{k} = k + \dfrac{1}{\beta(\Delta t)^2}m + \dfrac{\gamma}{\beta\Delta t}c$

2.0 *Calculations for each time step, $i = 0, 1, 2, \ldots$*

2.1 $\Delta\hat{P}_i = \Delta P_i + \left[\dfrac{1}{2\beta}m + \Delta t\left(\dfrac{\gamma}{2\beta} - 1\right)c\right]\ddot{x}_i + \left(\dfrac{1}{\beta\Delta t}m + \dfrac{\gamma}{\beta}c\right)\dot{x}_i$

2.2 $\Delta x_i = \dfrac{\Delta\hat{P}_i}{\hat{k}} \quad \Rightarrow \quad x_{i+1} = x_i + \Delta x_i$

2.3 $\Delta\dot{x}_i = \left(1 - \dfrac{\gamma}{2\beta}\right)\Delta t\ddot{x}_i - \dfrac{\gamma}{\beta}\dot{x}_i + \dfrac{\gamma}{\beta\Delta t}\Delta x_i \quad \Rightarrow \quad \dot{x}_{i+1} = \dot{x}_i + \Delta\dot{x}_i$

2.4 $\Delta\ddot{x}_i = \dfrac{1}{\beta(\Delta t)^2}\Delta x_i - \dfrac{1}{\beta\Delta t}\dot{x}_i - \dfrac{1}{2\beta}\ddot{x}_i \quad \Rightarrow \quad \ddot{x}_{i+1} = \ddot{x}_i + \Delta\ddot{x}_i$

3.0 *Move to the next time step. Set $i + 1$ to i and repeat from Step 2.1.*

4.1.2 Nonlinear Material Properties

For linear systems, implementing Newmark-β method is relatively straightforward. Newmark-β method can be applied to nonlinear systems but additional computations are needed. For nonlinear material behaviour, the equation of motion would have to be modified to

$$m\ddot{x} + c\dot{x} + f_s(x) = P(t) \tag{4.35}$$

where the spring force f_s is now nonlinearly related to the displacement x. Consider the nonlinear spring behaviour shown in Figure 4.6.

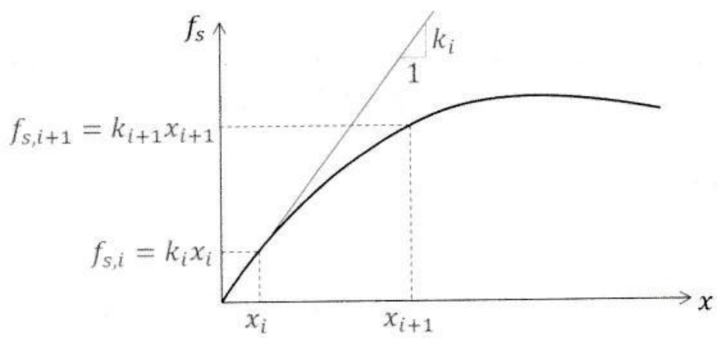

Figure 4.6 Nonlinear spring force

As can be seen, due to the varying stiffness, determining x_{i+1} becomes much more challenging. One approach to solving this problem is to use the *tangent stiffness* k_i at x_i and iteratively solving the dynamic equilibrium problem until the displacement approaches x_{i+1}, thereby, satisfying equilibrium at t_{i+1}. To do this, we need to add an additional calculation to calculate k_i at each time step, and use k_i in Equation 4.30. Nonlinear damping can be handled in a similar manner. Nonlinear systems will not be covered in this course.

4.1.3 First Order Methods

Rather than directly integrate second order equations, it is often easier to convert second order equations into a set of first order ordinary differential equations then integrate. Consider the equation of motion for forced vibration of a linear SDOF system.

$$m\ddot{x} + c\dot{x} + kx = P(t) \tag{4.36}$$

Solving for $\ddot{x}$, we get

$$\ddot{x} = \frac{P(t)}{m} - \frac{c\dot{x}}{m} - \frac{kx}{m} \tag{4.37}$$

Let

$$x_1 = x \tag{4.38a}$$

$$\dot{x}_1 = x_2 \tag{4.38b}$$

We can rewrite Equation 4.37 in terms of x_1 and x_2.

$$\dot{x}_2 = -\frac{c}{m}x_2 - \frac{k}{m}x_1 + \frac{1}{m}P(t) \tag{4.39}$$

Equation 4.38b and 4.39 can be written in matrix form as

$$\begin{bmatrix} \dot{x}_1 \\ \dot{x}_2 \end{bmatrix} = \begin{bmatrix} 0 & 1 \\ -\frac{k}{m} & -\frac{c}{m} \end{bmatrix} \begin{bmatrix} x_1 \\ x_2 \end{bmatrix} + \begin{bmatrix} 0 \\ \frac{1}{m} \end{bmatrix} P(t) \tag{4.40}$$

Equation 4.40 is the first order form of Equation 4.36, which can be readily solved in MATLAB™.

$\dot{z} = Az + Bu$ ← Input

Dynamics Matrix

State

Input Matrix

(State Space)

4.2 Earthquake Excitation

The time variation of the ground acceleration is the most useful way to define the ground motion due to an earthquake. Ground motion records are freely available electronically from many different databases such as the Pacific Earthquake Engineering Research Center (PEER) Ground Motion Database. There are many intricacies to analyzing and processing ground motion records but these are outside the scope of this course.

- Recall from our study of SDOF systems subjected to ground motion (Section 2.3.2), the equation of motion was

$$m\ddot{x} + c\dot{x} + kx = -m\ddot{x}_g \tag{4.41}$$

  where $\ddot{x}(t)$, $\dot{x}(t)$, and $x(t)$ are the acceleration, velocity, and displacement responses relative to the ground, respectively.
- The ground acceleration relative to the inertial reference frame, $\ddot{x}_g(t)$, appears on the right side of the equation. For a given ground acceleration, the problem is defined completely when the system's mass, stiffness, and damping are known properties.
- Figure 4.7 shows what is commonly referred to as the *El Centro* ground motion, so named because it was recorded at a site in El Centro, California during the Imperial Valley, California earthquake of May 18, 1940.

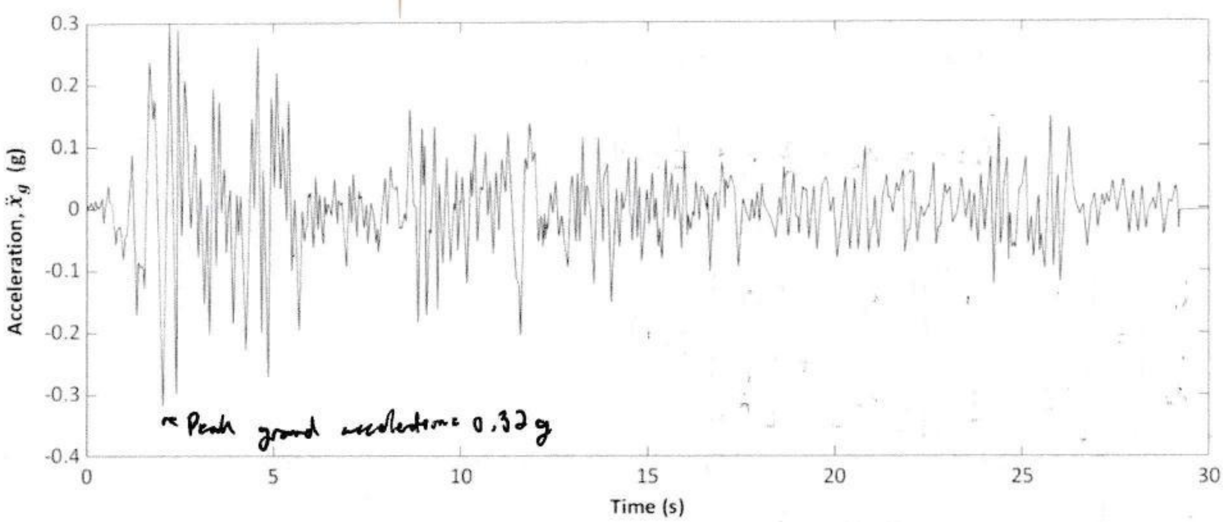

Figure 4.7 North-south component of horizontal ground acceleration recorded in El Centro, California during the Imperial Valley California earthquake on May 18, 1940

- The ground acceleration is defined by numerical values at discrete time instants. These time instants should be closely spaced to accurately capture the highly irregular variation acceleration with time. Typically, the time interval is 1/100 to 1/50 of a second.

- Acceleration is typically given in units of *g*, gravitational acceleration. The *peak ground acceleration* (PGA) in the El Centro ground motion is 0.319g.
- The equation of motion for earthquake ground motion in Equation 4.42 can be rearranged and expressed as

$$\ddot{x} + 2\zeta\omega_n\dot{x} + \omega_n^2 x = -\ddot{x}_g \tag{4.42}$$

- The response of a SDOF system to a given earthquake ground motion is dependant only on the natural frequency (period) and the damping of the system.
- Newmark-β method can be easily implemented to simulate the earthquake response of structures. The MATLAB™ script below can be used to analyze SDOF systems under earthquake excitation.

Newmark Method

```
clear all
close all
clc

% SDOF system definition
m=1; % Mass
Tn=1; % Natural period
wn=(2*pi)/Tn; % Circular natural frequency
z=0.02; % Damping ratio

elcentro=load('elcentro.dat'); % Ground motion
F=-m*elcentro*9.8; % Force vector

% Newmark-beta method parameters
g=0.5; % gamma
b=0.25; % beta
dt=0.02; % Time step size

% Initialization
c=2*wn*z*m; % Damping coefficient
k=wn^2*m; % Stiffness
d(1)=0; % Initial displacement
v(1)=0; % Initial velocity
a(1)=(F(1)-c*v(1)-k*d(1))/m; % Initial acceleration
khat=k+(1/(b*dt^2))*m+(g/(b*dt))*c;
A=(1/(2*b))*m+dt*(g/(2*b)-1)*c;
B=(1/(b*dt))*m+(g/b)*c;

for i=1:(length(F)-1)
  dFhat=(F(i+1)-F(i))+A*a(i)+B*v(i);
  dd=dFhat/khat;
  dv=dt*(1-g/(2*b))*a(i)-(g/b)*v(i)+(g/(b*dt))*dd;
```

```
    da=(1/(b*dt^2))*dd-(1/(b*dt))*v(i)-(1/(2*b))*a(i);
    d(i+1)=d(i)+dd;
    v(i+1)=v(i)+dv;
    a(i+1)=a(i)+da;
end
```

The response for the SDOF to the El Centro ground motion is plotted in Figure 4.8 for several natural frequencies and damping levels.

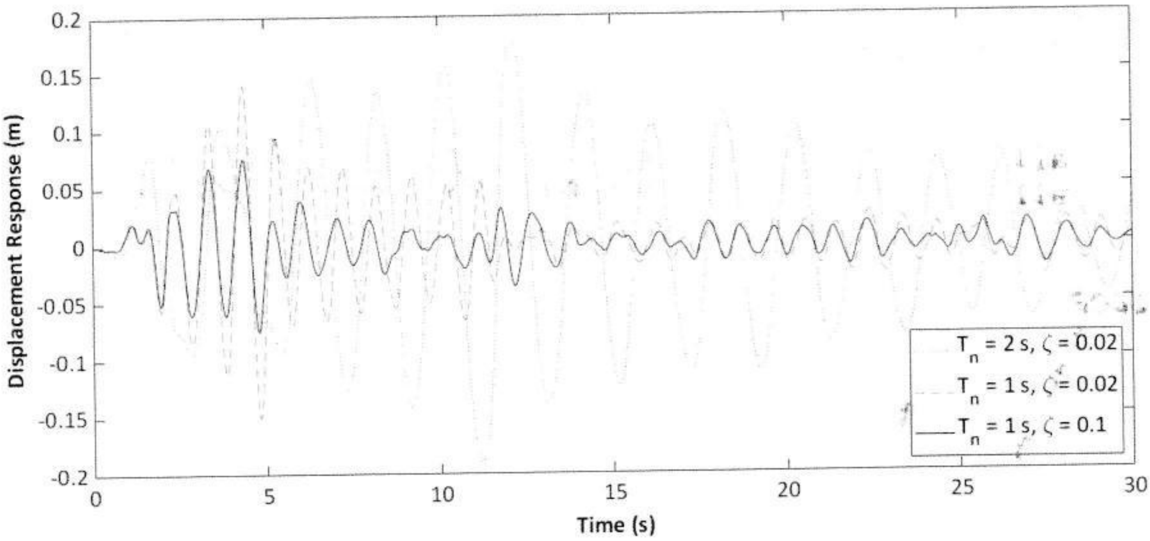

Figure 4.8 Response of a SDOF system to El Centro ground motion for various natural frequencies and damping ratios

4.2.1 Equivalent Static Force

For structural design, deformations, or the displacement of the structure relative to the ground, $x(t)$, are of primary interest.

- Deformations are linearly related to the internal forces in a structure.
- Consider a typical shear beam representation of a one-storey frame structure.

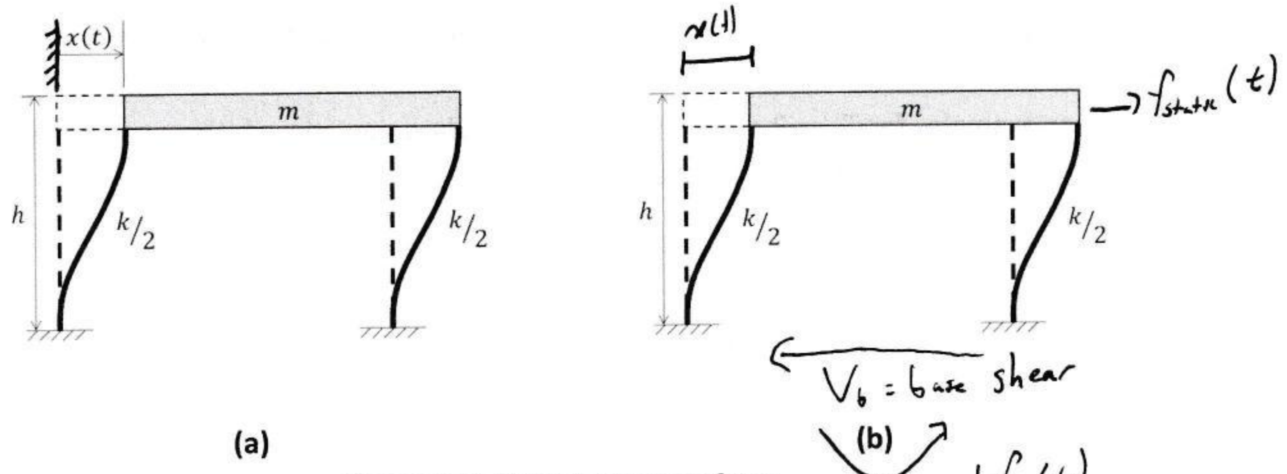

Figure 4.9 Equivalent static force

- The *equivalent static force* is the static force that must be applied to produce the same deformation $x(t)$ at time t.

$$f_{s_{static}}(t) = k x(t) \tag{4.43}$$

where k is the lateral stiffness of the frame.

- Once the static force $f_s(t)$ is determined, the base shear and base overturning moment can be found by a static analysis at each time instant. For the one-storey lateral frame, the base shear and overturning moment are

$$V_b(t) = f_{static}(t) \qquad (4.44a) \qquad\qquad M_b(t) = h f_{static}(t) \qquad (4.44b)$$

where h is the height of the mass above the base.

- The maximum value of the equivalent static force can be used to determine the maximum base shear and base overturning moment during the event.

4.3 Elastic Response Spectrum

The response spectrum is perhaps the most important concept in the design of structures to withstand earthquake loading.

RS = plot of peak response as a function of a natural frequency parameter (typ natural period)

We will investigate how to construct the deformation response spectrum for El Centro ground motion seen earlier.

- For example, for $T_n = 2$ s and $\zeta = 2\%$, the displacement time history computed using Nemark's method is plotted in Figure 4.10.

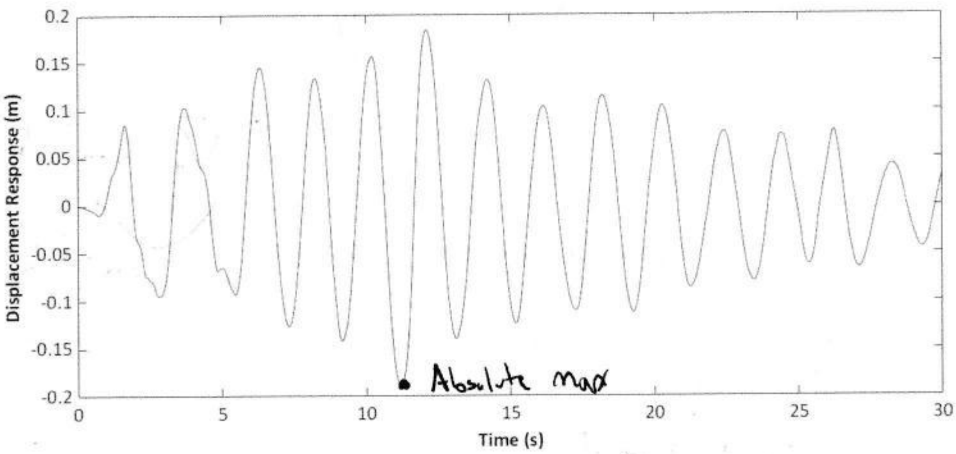

Figure 4.10 Displacement response to El Centro ground motion for SDOF system with $T_n = 2$ s and $\zeta = 2\%$

- The peak value, also called the *spectral displacement*, is

$$S_d = \max\Big(\text{abs}\big(x(t \mid T_n = 2\text{ s}, \zeta = 0.02)\big)\Big) = 0.1895\ m$$

  and occurs at $t = 11.2$ s.

- This procedure is repeated for a range of natural periods, T_n, and the peak response for is plotted against T_n. The resulting plot is known as the *deformation response spectrum*. The deformation spectrum for the El Centro ground motion is shown in Figure 4.11.

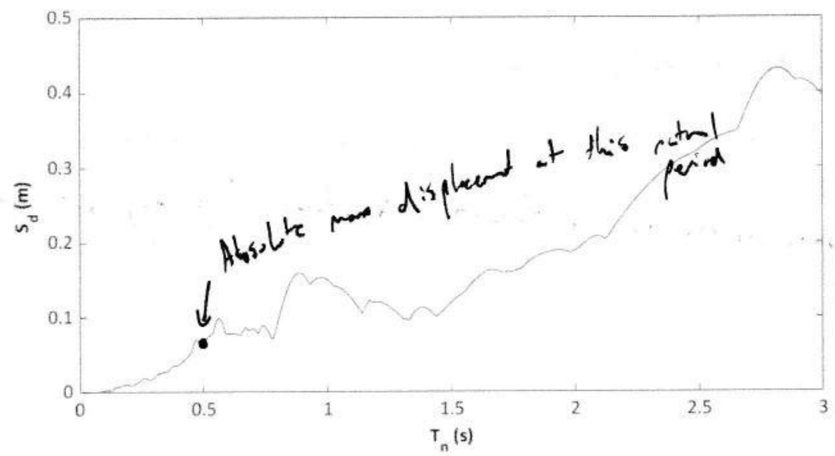

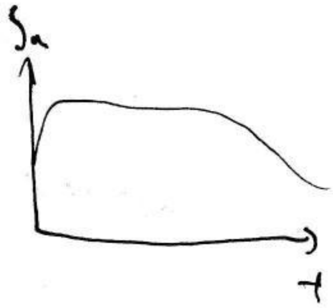

Figure 4.11 Elastic deformation response spectrum for El Centro ground motion for $\zeta = 2\%$

4.3.1 Pseudo- Velocity and Pseudo-Acceleration Spectra – Great as long as damping less than 10%.

As the prefix suggests, *pseudo-velocity* and *pseudo-acceleration* spectra do not represent the true response of a structure. Instead, they are related to the spectral displacement S_d through

Pseudo – Velocity

Pseudo – Acceleration

ω_n ; rads/sec
S_d = m
since rads not too concrete, $S_v \sim$ m/s (velocity)

$$S_v = \omega_n S_d = \frac{2\pi}{T_n} S_d \qquad (4.45a)$$

$$S_a = \omega_n^2 S_d = \left(\frac{2\pi}{T_n}\right)^2 S_d \qquad (4.45b)$$

- The pseudo quantities have the correct units of velocity and acceleration, and for most structures with reasonable damping, they provide close approximations of the true response.
- The pseudo-velocity and pseudo-acceleration spectra for the El Centro ground motion are shown in Figure 4.12 for $\zeta = 2\%$.

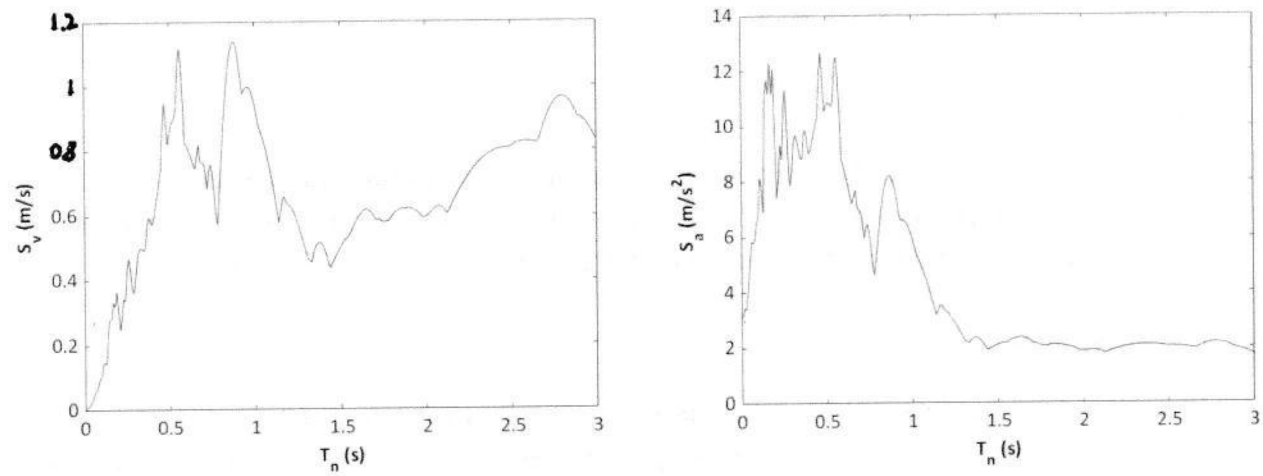

(a) **(b)**

Figure 4.12 Pseudo spectra for El Centro ground motion for $\zeta = 2\%$
(a) Pseudo-velocity **(b)** Pseudo-acceleration

- Consider the expression for the equivalent static force discussed earlier. We can determine the maximum equivalent lateral force in an earthquake as

$$f_{s\,max} = k|x(t)|_{max} = k S_d = k\, S_a/\omega_n^2 = m S_a \qquad (4.46)$$

MAX EQUIVALENT LATERAL FORCE

- For structural design purposes, we can also compute the maximum base shear as

$$V_{b,max} = f_{s,max}$$
$$= m S_a$$
$$= \frac{W}{g} S_a = \frac{S_a}{g} W$$

Base shear coefficient

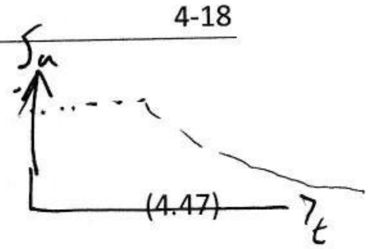

(4.47)

where W is the weight of the structure and g is the acceleration due to gravity. The non-dimensional ratio S_a/g is called the *base shear coefficient* or *lateral force coefficient*. It is used in building codes to represent the coefficient by which the structural weight is multiplied to obtain the peak base shear.

- Physically, the pseudo-velocity is related to the strain energy stored in the elastic elements of the structure. The maximum strain energy stored in the system is given by

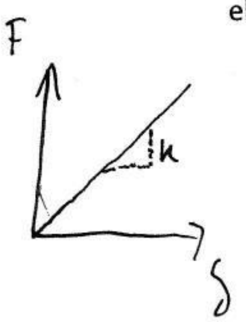

$$V = \frac{1}{2} k S_d^2$$
$$= \frac{1}{2} m S_v^2 \qquad (4.48)$$

- It must be emphasized that we only need to generate the deformation response spectrum, and the pseudo-velocity and the pseudo-acceleration spectra can be obtained by multiplying the values of the spectral displacement, S_d, by ω_n and ω_n^2, respectively.

4.3.2 Tripartite Plot

The tripartite plot, also referred to as the combined D-V-A spectrum, is a compact, convenient way to plot the deformation, pseudo-velocity, and pseudo-acceleration spectra on the same graph. This is enabled by the fact that these three quantities are scalar multiples of each other. In tripartite plots, S_d, S_v, and S_a presented on a four-way logarithmic graph. The combined spectrum for the El Centro ground motion is shown in Figure 4.13.

- S_v is read off the vertical axis while S_d and S_a are on the diagonal axes sloping at +45° and -45° from the T_n-axis, respectively.
- In general, earthquake response spectra are very irregular. However, they are characterized by a general trapezoidal (tent) shape
- It is important to note that response spectra are earthquake-specific. Ground motion characteristics are affected by many different factors including earthquake magnitude, fault-to-site-distance, source-to-site geology, and the soil conditions at the site.
- As a result, different earthquakes recorded at the same site can yield distinctly different response spectra.

Very stiff Typical stiffness Not too stiff

Acceleration Sensitive | Velocity Sensitive | Displacement Sensitive Region

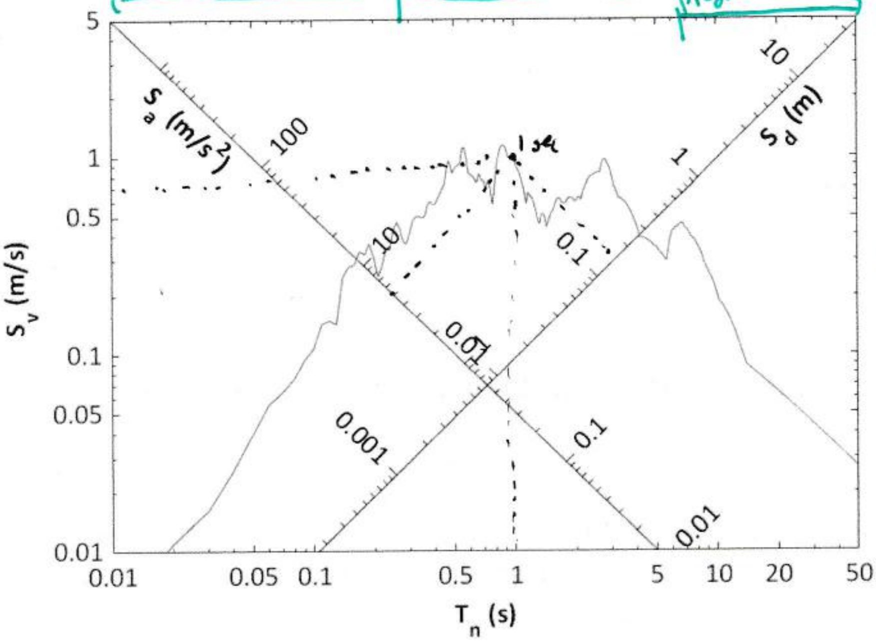

General Shape

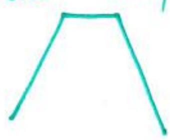

Figure 4.13 Combined deformation, pseudo-velocity, and pseudo-acceleration response spectrum for El Centro ground motion for $\zeta = 2\%$

Example 4.2 Determine the maximum equivalent static force for the frame show in Figure 4.14 subjected to El Centro ground motion. Assume 2% critical damping.

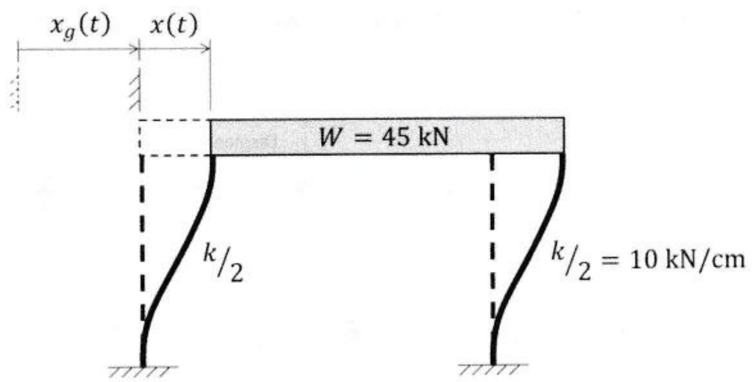

Figure 4.14 Lateral frame subjected to El Centro ground motion

Solution: The natural frequency of the frame for the lateral mode is

The peak displacement can be obtained from the tripartite plot in Figure 4.13 or the deformation spectrum in Figure 4.11

The maximum equivalent static force is

4.4 Earthquake Response of Linear MDOF Systems

Analysis of the earthquake response of linear MDOF systems can take two approaches.

- *Response history analysis* (RHA) is an accurate method which gives the response of a structure over time to the application of ground motion. It is able to accommodate general cases of structures and excitations.
- *Response spectrum analysis* seeks to compute the peak response of a structure directly from the earthquake response spectrum without the need for a response history analysis. The approach is approximate and generally used for design purposes.

4.4.1 Response History Analysis

Consider the general MDOF structure shown below in which the mass is lumped at the joints or nodes and each node has three degrees-of-freedom, two translational and one rotational.

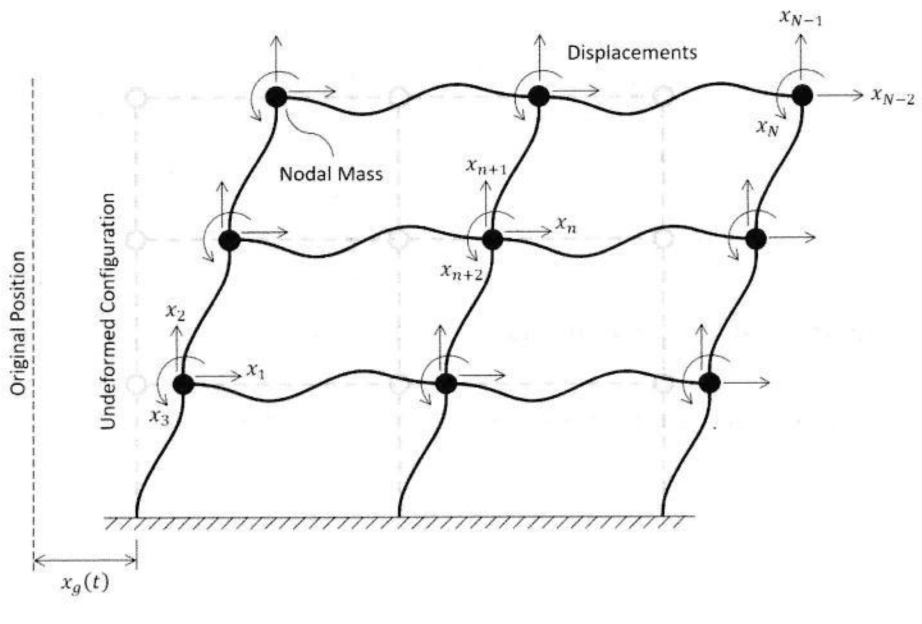

Figure 4.15 Plane frame modelled as a MDOF system subjected to earthquake ground motion

ground motion, only influences the horizontal DOF (1's)

relative displacement

We can write the absolute displacements $\boldsymbol{x}_t(t)$ as

$$\vec{x}_t(t) = \begin{bmatrix} x_1(t) \\ x_2(t) \\ x_3(t) \\ \vdots \\ x_{N-2}(t) \\ x_{N-1}(t) \\ x_N(t) \end{bmatrix} + x_g \begin{bmatrix} 1 \\ 0 \\ 0 \\ \vdots \\ 1 \\ 0 \\ 0 \end{bmatrix} = \vec{x} + \vec{R}\, x_g(t) \tag{4.49}$$

where $\boldsymbol{R}$ is a $N \times 1$ vector containing ones and zeros, known as the *influence vector* which defines the displacements induced in a structure when the base is subjected to ground motion. It follows then,

$$\dot{x}_t = \dot{x} + R\dot{x}_g \tag{4.50}$$

and the equation of motion can be written as

$$\ddot{x}_t = \ddot{x} + R\ddot{x}_g, \quad M_{N\times N}\ddot{x}_{N\times 1} + C_{N\times N}\dot{x}_{N\times 1} + K_{N\times N}x_{N\times 1} = -M_{N\times N}R_{N\times 1}\ddot{x}_g \tag{4.51}$$

In the ensuing study, we will assume that the modes are mass normalized, the damping matrix $\boldsymbol{C}$ is proportional, and that the mass and stiffness matrices are in the form of a lumped mass shear beam approximation model. Using the modal transformation

$$\boldsymbol{x} = \boldsymbol{\Phi y} \tag{4.52}$$

and pre-multiplying Equation 4.51 by

big gamma

$$\begin{gathered} \boldsymbol{\Phi}^T\boldsymbol{M\Phi\ddot{y}} + \boldsymbol{\Phi}^T\boldsymbol{C\Phi\dot{y}} + \boldsymbol{\Phi}^T\boldsymbol{K\Phi y} = -\boldsymbol{\Phi}^T\boldsymbol{MR}\ddot{x}_g \\ \mathbf{I}\boldsymbol{\ddot{y}} + \boldsymbol{\Phi}^T\boldsymbol{C\Phi\dot{y}} + \boldsymbol{\Omega}^2\boldsymbol{y} = -\boldsymbol{\Gamma}\ddot{x}_g \end{gathered} \tag{4.53}$$

Introducing the parameter $\boldsymbol{\Gamma} = \boldsymbol{\Phi}^T\boldsymbol{MR}$, or $\Gamma_i = \boldsymbol{\phi}_i^T\boldsymbol{MR}$, we get

Modal Participation Factor

↳ How significant each mode is to the response of the system

$$\ddot{y}_1 + 2\zeta_1\omega_{n,1}\dot{y}_1 + \omega_{n,1}^2 y_1 = -\Gamma_1\ddot{x}_g \tag{4.54a}$$

$$\ddot{y}_2 + 2\zeta_2\omega_{n,2}\dot{y}_2 + \omega_{n,2}^2 y_2 = -\Gamma_2\ddot{x}_g \tag{4.54b}$$

$$\vdots$$

$$\ddot{y}_N + 2\zeta_N\omega_{n,N}\dot{y}_N + \omega_{n,N}^2 y_N = -\Gamma_N\ddot{x}_g \tag{4.54c}$$

Γ_i is known as the *modal participation factor* but this is a somewhat misleading name since Γ_i depends on modes are normalization. As a result, the relative values of Γ_i by themselves may not provide a measure of the contribution of mode i to a response quantity. To understand how significant mode i is to the overall response, we need to compare the modal responses directly.

Recall from the study of the response of SDOF systems to ground motion, we numerically evaluated the response of the following SDOF system:

$$
\begin{aligned}
m\ddot{u} + c\dot{u} + ku &= -m\ddot{u}_g \\
\ddot{u} + 2\zeta\omega_n\dot{u} + \omega_n^2 u &= -\ddot{u}_g
\end{aligned}
\tag{4.55}
$$

Comparing Equation 4.55 to one of the uncoupled equations in Equations 4.54, we see that the modal response y_1, y_2, ..., y_N can be obtained by multiplying the response using Equation 4.55 by the corresponding Γ_i. Therefore, the i^{th} modal response is given by

$y_i(t) = \Gamma_i u_i(t)$ ← unscaled, then scaled directly (4.56)

where $\Gamma_i = \boldsymbol{\phi}_i^T \boldsymbol{M}\boldsymbol{R}$ and $u_i(t)$ is the response (or solution) of the following SDOF system:

$$
\ddot{u}_i + 2\zeta_i\omega_{n,i}\dot{u}_i + \omega_{n,i}^2 u_i = -\ddot{u}_g
\tag{4.57}
$$

The SDOF problem can be easily solved using Newmark-β method as demonstrated in Section 4.2. We can then transform the i^{th} mode response back to physical coordinates to obtain its contribution to the total response

$$
\boldsymbol{x}_i(t) = \boldsymbol{\phi}_i y_i(t) = \boldsymbol{\phi}_i \Gamma_i u_i(t)
\tag{4.58}
$$

The total response in physical coordinates is the sum of the contributions from all N modes.

$$
\begin{aligned}
\boldsymbol{x}(t) &= \sum_{i=1}^{N} \boldsymbol{x}_i(t) \\
&= \sum_{i=1}^{N} \boldsymbol{\phi}_i \Gamma_i u_i(t)
\end{aligned}
\tag{4.59}
$$

Example 4.3 Analyze the displacement response of the three-storey shear building shown below to the El Centro ground motion. Assume 5% classical damping in each mode.

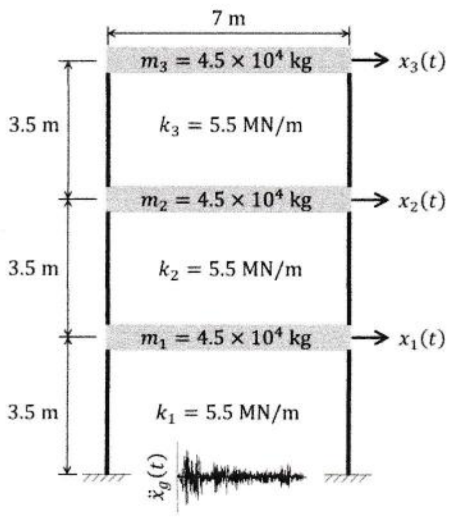

$$
\boldsymbol{M} = 10^4 \begin{bmatrix} 4.5 & 0 & 0 \\ 0 & 4.5 & 0 \\ 0 & 0 & 4.5 \end{bmatrix} \text{kg}
$$

$$
\boldsymbol{K} = \begin{bmatrix} 11 & -5.5 & 0 \\ -5.5 & 11 & -5.5 \\ 0 & -5.5 & 5.5 \end{bmatrix} \text{MN/m}
$$

Solution: The equation of motion is given by

$$M\ddot{x} + C\dot{x} + Kx = -M\iota\ddot{x}_g$$
$$= -M\begin{bmatrix}1\\1\\1\end{bmatrix}\ddot{x}_g$$

The natural frequencies and mode shapes obtained from solving the eigenvalue problem are summarized below.

	Mode 1	Mode 2	Mode 3
Natural Frequency (rad/s)	4.92	13.79	19.92
Natural Period (s)	1.28	0.46	0.32
Mode Shape Vector (Mass Normalized)	$\phi_1 \begin{bmatrix}0.0015\\0.0028\\0.0035\end{bmatrix}$	$\phi_2 \begin{bmatrix}-0.0035\\-0.0015\\0.0028\end{bmatrix}$	$\phi_3 \begin{bmatrix}0.0028\\-0.0035\\0.0015\end{bmatrix}$

Decouple the system into three SDOF systems by transforming the equation of motion into modal coordinates.

$$\ddot{y}_1 + 2\zeta_1\omega_{n,1}\dot{y}_1 + \omega_{n,1}^2 y_1 = -\Gamma_1\ddot{x}_g$$
$$\ddot{y}_2 + 2\zeta_2\omega_{n,2}\dot{y}_2 + \omega_{n,2}^2 y_2 = -\Gamma_2\ddot{x}_g$$
$$\ddot{y}_3 + 2\zeta_3\omega_{n,3}\dot{y}_3 + \omega_{n,3}^2 y_3 = -\Gamma_3\ddot{x}_g$$

Modal participation factors

$$\Gamma_i = \boldsymbol{\phi}_i^T \boldsymbol{MR}$$

$$= [0.0015, 0.0028, 0.0035]\begin{bmatrix}4.5\times10^4 & & \\ & 4.5\times10^4 & \\ & & 4.5\times10^4\end{bmatrix}\begin{bmatrix}1\\1\\1\end{bmatrix}$$

$$1 = 351.28$$

$$\Gamma_2 = \boldsymbol{\phi}_2^T \boldsymbol{MR} = -100.54 \qquad \Gamma_3 = \boldsymbol{\phi}_3^T \boldsymbol{MR} = 38.61$$

The SDOF equations can be easily solved using the Newmark-β method MATLAB™ code on Page 4-13. The responses in modal coordinates are plotted below.

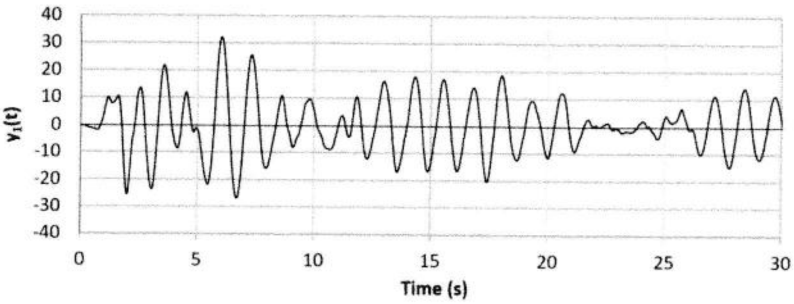

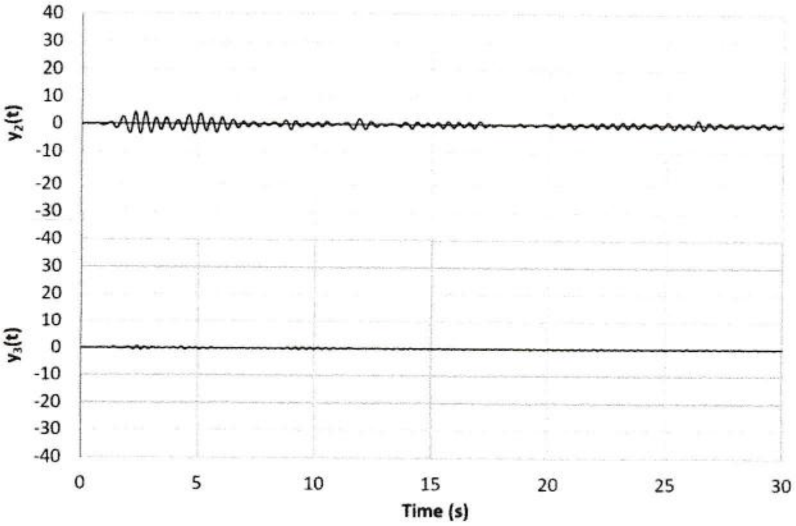

The displacement response in physical coordinates is given by

$$x(t) = \begin{bmatrix} x_1(t) \\ x_2(t) \\ x_3(t) \end{bmatrix} = \sum_{i=1}^{3} x_i = \sum_{i=1}^{3} \phi_i y_i(t)$$

The displacement response time history is shown below.

Do not always occur at the same time

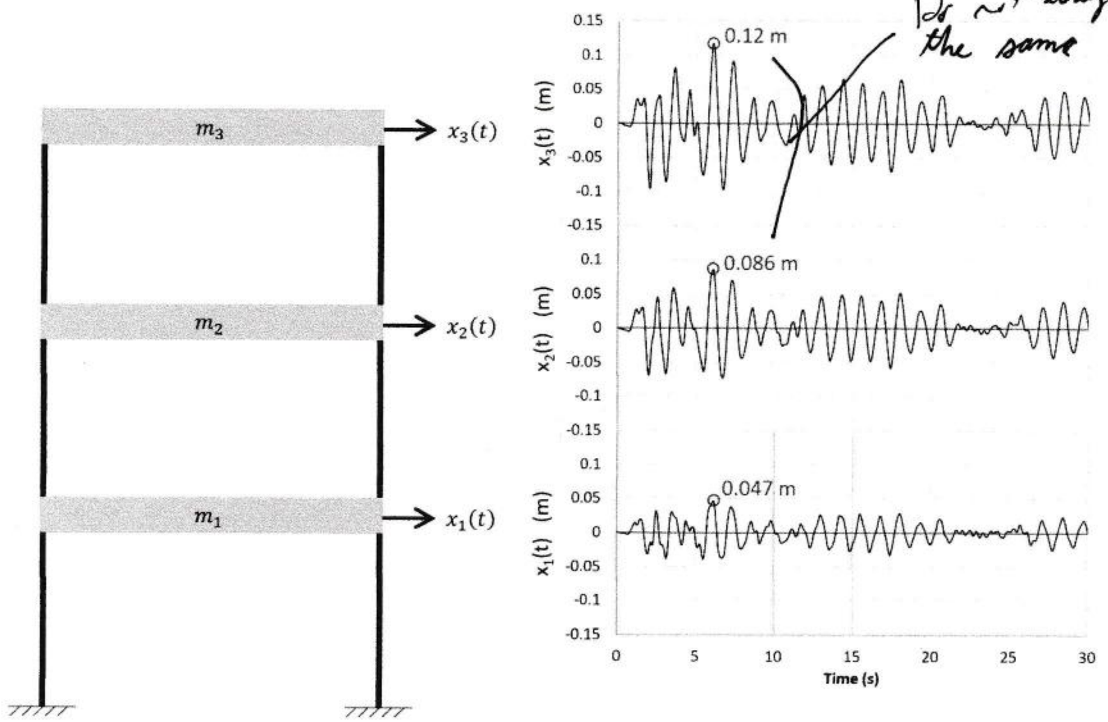

4.4.2 Response Spectrum Method

Dynamic time history analysis is perhaps the most natural way to analyze the response of a structure but it can be very cumbersome for MDOF structures. Moreover, we may not be interested in the overall response of the structure, especially if it is expected to remain elastic. If we have the response spectra for an earthquake we can conveniently and expeditiously estimate the maximum response of a MDOF structure using the *response spectrum method*.

As we have developed above, an MDOF system can be decomposed into a series of uncoupled SDOF systems through modal transformation. The peak displacement response in the i^{th} mode is simply,

$$\max\left[\vec{r}_i(t)\right] = \vec{\phi}_i \Gamma_i \max\left[y_i(t)\right] = \phi_i \Gamma_i S_d \tag{4.59}$$

where $S_d(T_i, \zeta_i)$ denotes the response spectrum ordinate. Alternatively, using the acceleration response spectrum,

$$\max\left[x(t)\right] = \phi_i \Gamma_i \frac{S_a}{\omega_{n,i}^2} = \phi_i \Gamma_i \left(\frac{T_{n,i}}{2\pi}\right)^2 S_a \tag{4.60}$$

These equations are convenient, however, it is important to note that the maximum modal responses do not necessarily occur exactly at the same time instant and the response spectra do not provide information about when the maximum response occurs. Therefore, directly superposing the maximum modal responses does not yield the true peak structural response.

To overcome this problem, researchers have developed approximate relationships or rules to combine the modal responses. Here, we will only discuss two simple rules. Since these rules can be used for any response parameter such as displacement, velocity, acceleration or internal force, we will express them in terms of a general vector $\boldsymbol{r}(t)$.

Absolute Sum (ABSSUM) Rule The simplest way to approximate the maximum response of a system is to directly sum the absolute values of the modal responses.

doesn't care that they occur at different ~~times~~ times

$$\max[\boldsymbol{r}(t)] = \sum_{i=1}^{N} \max\ |\boldsymbol{r}_i(t)| \tag{4.61}$$

The ABSSUM rule yields an upper bound to the true maximum response because it assumes that all the modal maxima occur at the same time with the same sign. However, it is generally too conservative for practical purposes.

Square Root of the Sum of Squares (SRSS) Rule First introduced in 1953 by L. E. Goodman, E. Rosenblueth, and N. M. Newmark, the SRSS rule is still widely used in practice.

~~max[r(t)]~~

$$\max\left[\vec{r}(t)\right] = \sqrt{\sum_{i=1}^{N} \left(\max\left[r_i(t)\right]\right)^2} \tag{4.62}$$

The SRSS rule yields accurate results for regular, flexible structures with no irregularities in plan or elevation but not for structures with closely spaced natural frequencies. Closely spaced natural frequencies occur commonly in buildings with torsional modes, buildings with appendages, and soil-structure systems. The SRSS rule is also inaccurate when applied to structures with significant higher modes as the responses in high frequency modes are strongly correlated with those of low frequency modes.

Example 4.4 Use the SRSS rule to determine the maximum roof displacement, peak base shear, and overturning moment for the building in Example 4.3. The 5% damped pseudo-acceleration spectrum for the El Centro ground motion is provided below.

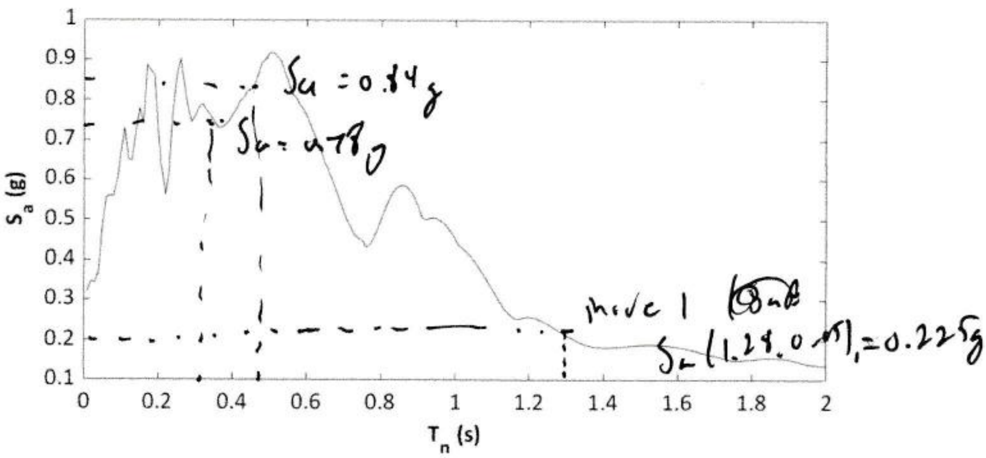

Solution: From Example 4.3,

	Mode 1	Mode 2	Mode 3
Natural Frequency (rad/s)	4.92	13.79	19.92
Natural Period (s)	1.28	0.46	0.32
Mode Shape Vector (Mass Normalized)	$\begin{bmatrix} 0.0015 \\ 0.0028 \\ 0.0035 \end{bmatrix}$	$\begin{bmatrix} -0.0035 \\ -0.0015 \\ 0.0028 \end{bmatrix}$	$\begin{bmatrix} 0.0028 \\ -0.0035 \\ 0.0015 \end{bmatrix}$
Mode Participation Factor	351.28	-100.54	38.61

We can determine the acceleration from the given response spectrum and compute the maximum modal displacement response using

$$\max[\boldsymbol{x}_i(t)] = \boldsymbol{\phi}_i \Gamma_i \left(\frac{T_{n,i}}{2\pi}\right)^2 S_a(T_i, \zeta_i)$$

	Mode 1	Mode 2	Mode 3
Acceleration (g)	0.23	0.84	0.78

Acceleration (m/s²) 2.76 8.24 7.55

$\max[\boldsymbol{x}_i(t)]$

Peak displacement vector $= \begin{bmatrix} 0.051 \\ 0.091 \\ 0.114 \end{bmatrix}$ m $\quad \begin{bmatrix} 0.015 \\ 0.007 \\ -0.012 \end{bmatrix}$ m $\quad \begin{bmatrix} 0.002 \\ -0.003 \\ 0.001 \end{bmatrix}$

Peak displacement using the SRSS rule:

$$\max[\boldsymbol{x}(t)] = \sqrt{\sum_{i=1}^{N}(\max[\boldsymbol{x}_i(t)])^2} = \begin{bmatrix} \sqrt{0.051^2 + 0.015^2 + 0.002^2} \\ \sqrt{0.091^2 + 0.007^2 + 0.003^2} \\ \sqrt{0.114^2 + 0.012^2 + 0.001^2} \end{bmatrix} = \begin{bmatrix} 0.053 \\ 0.092 \\ 0.115 \end{bmatrix} \text{ m}$$

It can be seen that the SRSS rule yields reasonably close approximations compared to the results in Example 4.3.

To estimate the peak base shear and overturning moment, we must first compute the equivalent static forces corresponding to the maximum displacements. The maximum equivalent static force in each of the three modes is given by

$$\max[\boldsymbol{F}_i(t)] = \boldsymbol{K}\max[\boldsymbol{x}_i(t)]$$

$M\phi_i \Gamma_i S_a$ peak modal displacement ✓ peak static force

$$\max[\boldsymbol{F}_1(t)] = \begin{bmatrix} 11 & -5.5 & 0 \\ -5.5 & 11 & -5.5 \\ 0 & -5.5 & 5.5 \end{bmatrix}\begin{bmatrix} 0.051 \\ 0.091 \\ 0.114 \end{bmatrix} = \begin{bmatrix} 0.055 \\ 0.100 \\ 0.124 \end{bmatrix} \text{ MN}$$

$$\max[\boldsymbol{F}_2(t)] = \begin{bmatrix} 11 & -5.5 & 0 \\ -5.5 & 11 & -5.5 \\ 0 & -5.5 & 5.5 \end{bmatrix}\begin{bmatrix} 0.015 \\ 0.007 \\ -0.012 \end{bmatrix} = \begin{bmatrix} 0.130 \\ 0.058 \\ -0.104 \end{bmatrix} \text{ MN}$$

$$\max[\boldsymbol{F}_3(t)] = \begin{bmatrix} 11 & -5.5 & 0 \\ -5.5 & 11 & -5.5 \\ 0 & -5.5 & 5.5 \end{bmatrix}\begin{bmatrix} 0.002 \\ -0.003 \\ 0.001 \end{bmatrix} = \begin{bmatrix} 0.037 \\ -0.046 \\ 0.021 \end{bmatrix} \text{ MN}$$

The base shear and overturning moment for each mode can be determined from statics

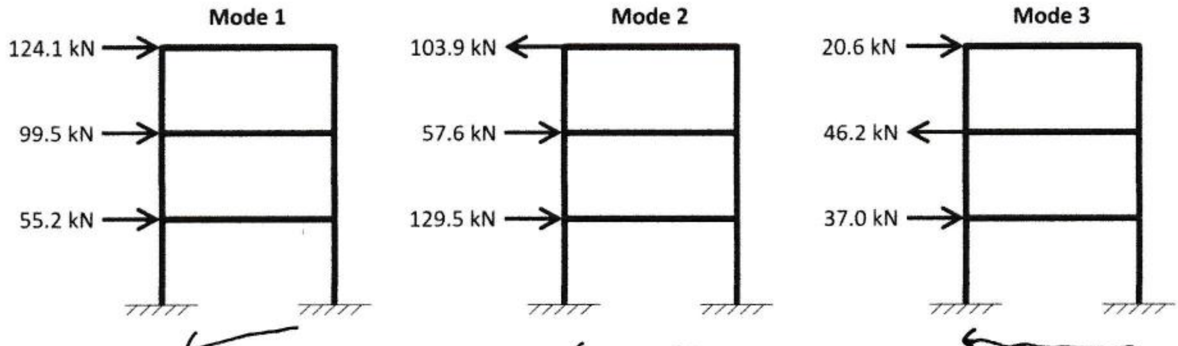

$V_{b,1} = 278.8$ kN $\quad V_{b,2} = 83.2$ kN $\quad$ 11.4

2192.8 $\quad$ 234.5 kNm $\quad M_{o,3} = 146.1$ kNm

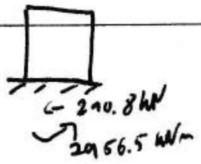

Peak base shear using the SRSS rule:

$$\max[V_b(t)] = \sqrt{\sum_{i=1}^{N}\left(\max[V_{b,i}(t)]\right)^2} = \sqrt{278.8^2 + 83.2^2 + 11.4^2} = 290.8\text{ kN}$$

Peak overturning moment using the SRSS rule:

$$\max[M_b(t)] = \sqrt{\sum_{i=1}^{N}\left(\max[M_{b,i}(t)]\right)^2} = \sqrt{2192.8^2 + 234.5^2 + 1969.1^2} = 2956.5\text{ kN}\cdot\text{m}$$

4.4.3 Equivalent Static Method

In practice, detailed numerical modelling of structures is generally avoided whenever possible. Even the response spectrum method can become unwieldly for large structures. The *equivalent static method* is a much more simplified and convenient alternative. Let us take a closer look at what we saw in Example 4.4. The equivalent static force associated with the i^{th} mode is

$$F_i(t) = K x_i(t) \tag{4.63}$$

where $\boldsymbol{K}$ is the assembled stiffness matrix and $\boldsymbol{F}_i(t)$ are the equivalent static forces producing the same displacements as the i^{th} mode responses, $\boldsymbol{x}_i(t)$ at each time instant t. The maximum equivalent static forces in the i^{th} mode of the structure are given by

$$\begin{aligned}\max[\boldsymbol{F}_i(t)] &= \boldsymbol{K}\max[\boldsymbol{x}_i(t)] = \boldsymbol{K}S_d(T_{n,i},\zeta_i)\\ &= \boldsymbol{K}\boldsymbol{\phi}_i\Gamma_i\left(\frac{T_{n,i}}{2\pi}\right)^2 S_a(T_{n,i},\zeta_i)\end{aligned} \tag{4.64}$$

Using the eigenequation in Equation 3.48, we can rewrite Equation 4.64 as

$$\max[F_i(t)] = M\phi_i\Gamma_i S_a(T_{n,i},\zeta_i) \tag{4.65}$$

If the mass matrix, $\boldsymbol{M}$, is diagonal,

$$\begin{bmatrix}F_{1,i}\\ F_{2,i}\\ F_{N,i}\end{bmatrix} \qquad \max[\boldsymbol{F}_i(t)] = \begin{bmatrix}m_1\phi_{1i}\\ m_2\phi_{2i}\\ \vdots\\ m_N\phi_{Ni}\end{bmatrix}\Gamma_i S_a(T_{n,i},\zeta_i) \tag{4.66}$$

For the i^{th} mode, the peak equivalent static force acting on the j^{th} mass is then,

$$F_{j,i} = \max[F_{j,i}(t)] = m_j\phi_{j,i}\Gamma_i S_a(T_{n,i},\zeta_i) \tag{4.67}$$

Consider the N-storey shear frame building shown in Figure 4.16. The base shear in the i^{th} mode of vibration is the sum of the static forces

$$V_{b,i} = \sum_{j=1}^{N} F_{j,i}$$

$$= S_a(T_{n,i}, \zeta_i)\Gamma_i \sum_{j=1}^{N} m_j \phi_{j,i} \qquad (4.68)$$

$$= \frac{S_a(T_{n,i}, \zeta_i)}{g}\Gamma_i \sum_{j=1}^{N} w_j \phi_{j,i} = \frac{S_a}{g} W_i^*$$

where g is the acceleration of gravity and w_j is the weight of the building's j^{th} floor.

S_a/g: base shear coefficient

$$W_i^* = \Gamma_i \sum_{j=1}^{N} w_j \phi_{j,i} \qquad (4.69)$$

is known as the *effective weight* of the structure in the i^{th} mode and represents the fraction of the total weight of the structure that participates in that mode of vibration. $w = N$, $m = kg$

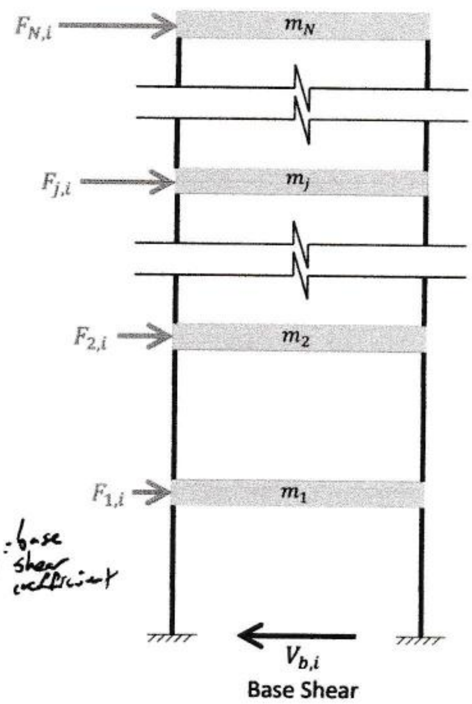

Figure 4.16 i^{th} mode equivalent static forces and base shear in an N-storey shear frame building

Using Equation 4.67 and 4.69, we can write the equivalent lateral forces in terms of the modal base shear as

Ignores all higher modes than fundamental mode

$$F_{j,i} = \frac{m_j \phi_{j,i}}{\sum_{j=1}^{N} m_j \phi_{j,i}} V_{b,i} \qquad (4.70)$$

To determine the modal base shear and modal equivalent lateral forces, however, we need to know the mode shapes and natural frequencies. If we use the actual mode shape vectors, we are back to the response spectrum method. To avoid having to solve the eigenvalue problem and simplify the analysis further, the following assumptions are made in classical equivalent static force procedures:

1. Structure only responding in fundamental mode (MODE 1)
2. Mode shape for fundamental mode varies linearly w/ height
3. Effective weight of Mode 1 equal to total weight of structure

These assumptions are generally valid for regular, conventional structures whose response does tend to be dominated by its fundamental mode in which the effective weight typically ranges between 60 and 80% of its total weight. Based on these assumptions we can approximate the base shear as → Assume $w_1^* = W$

$$V_b = V_{b,1} = \frac{W}{g} S_a\left[T_{n,1}, \Gamma_1 = 1\right] \tag{4.71}$$

The assumption of linearly varying mode shape yields ↙ Similar Triangles

$$\phi_{j,1} = \frac{\phi_{N,1}}{h_N} h_j \tag{4.72}$$

where h_N is the total height of the building and h_j denotes the height of the j^{th} floor of the building measured from the base . Finally, the lateral forces can be estimated as

$$F_{j,1} = \frac{w_j\left(\frac{\phi_{N,1}}{h_N} h_j\right)}{\sum_{j=1}^{N} w_j\left(\frac{\phi_{N,1}}{h_N} h_j\right)} V_{b,1}$$

$$F_{j,1} = \frac{w_j h_j}{\sum_{j=1}^{N} w_j h_j} V_{b,1} \tag{4.73}$$

Equation 4.73 only depends on the weight and height of the floors, and the response spectrum of the ground motion that excites the structure.

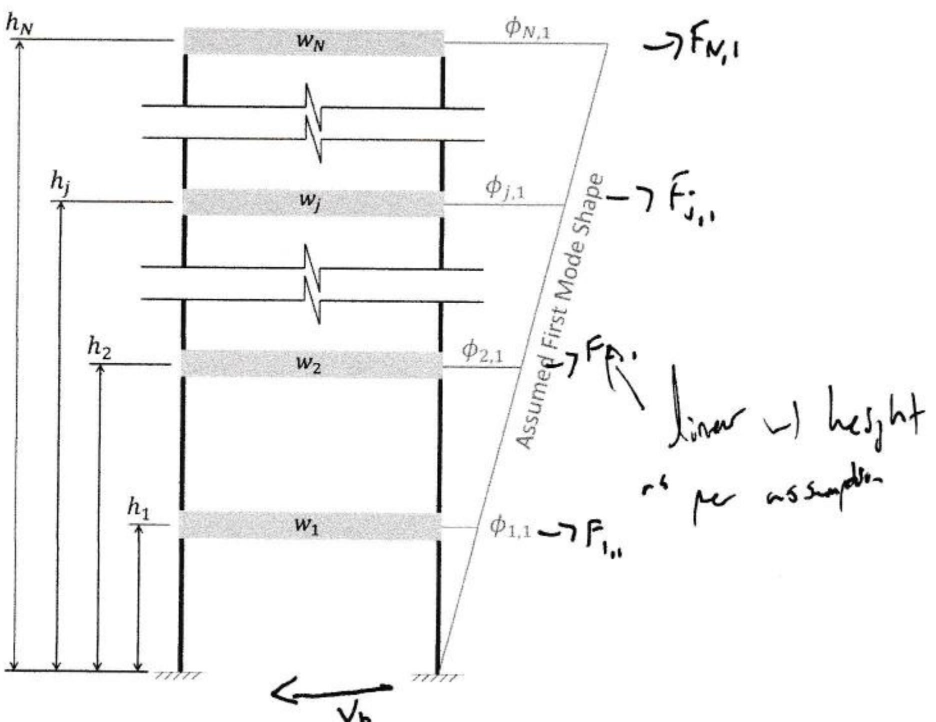

Figure 4.17 Assumed first mode shape in equivalent static force method

CHING
CHONG

MR. MEAN EUGENE

between 60 and 80% of its total weight. Based on these assumptions we can approximate the base shear as

(4.71)

The assumption of linearly varying mode shape yields

$$\phi_{j,1} = \frac{\phi_{N,1}}{h_N} h_j \tag{4.72}$$

where h_N is the total height of the building and h_j denotes the height of the j^{th} floor of the building measured from the base . Finally, the lateral forces can be estimated as

$$\begin{aligned} F_{j,1} &= \frac{w_j \left(\frac{\phi_{N,1}}{h_N} h_j\right)}{\sum_{j=1}^{N} w_j \left(\frac{\phi_{N,1}}{h_N} h_j\right)} V_{b,1} \\ &= \frac{w_j h_j}{\sum_{j=1}^{N} w_j h_j} V_{b,1} \end{aligned} \tag{4.73}$$

Equation 4.73 only depends on the weight and height of the floors, and the response spectrum of the ground motion that excites the structure.

CH
I
NG CHONG

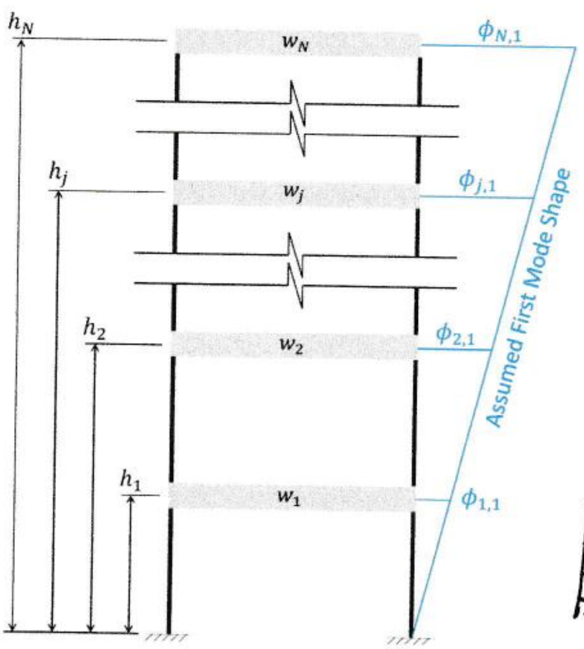

All good for regular structures


Walls - Regular


Walls - center of stiffness not in middle. ∴ Due to eccentricity is not [illegible]

Figure 4.17 Assumed first mode shape in equivalent static force method

The lateral forces are applied at the centre of mass of the building's floors in the direction of the ground motion being considered and the response of the building such as storey drifts and member internal forces can then be determined using any method that can be used to analyze structures under static loads.

Example 4.5 Use the equivalent static force method to estimate the base shear and overturning moment for the building in Example 4.3.

Solution: From Example 4.4,

$$S_a(T_{n,1} = 1.28\text{ s}, \zeta_1 = 0.05) = 2.26\text{ m/s}^2 = 0.23g$$

The total weight of the building is

$$W = (m_1 + m_2 + m_3) \times g = (3 \times 45{,}000\text{ kg}) \times 9.81\text{ m/s}^2 = 1324.35\text{ kN}$$

Base shear:

$$V_b = \frac{W}{g} S_a = \frac{1324350}{g}(0.23g) = 304.6\text{ kN}$$

The equivalent static force acting on each floor is given by

$$F_{j,1} = \frac{w_j h_j}{\sum_{j=1}^{N} w_j h_j} V_{b,1}$$

$$\sum_{j=1}^{N} w_j h_j = (45000 \times 9.81)(3.5 + 7.0 + 10.5)/1000 = 9270.45\text{ kN} \cdot \text{m}$$

Storey	w_j (kN)	h_j (m)	$\frac{w_j h_j}{\sum_{j=1}^{N} w_j h_j}$	$F_{j,1}$ (kN)
2	441.45	3.5	0.167	50.77
3	441.45	7.0	0.333	101.53
Roof	441.45	10.5	0.500	152.30

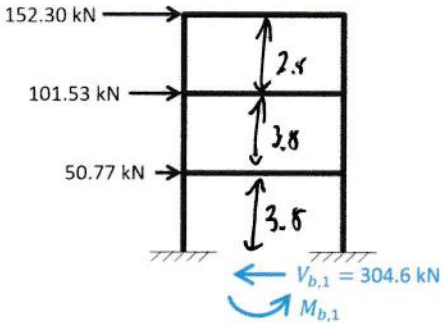

Overturning moment:

$$M_b = 152.3 \cdot 10.5 + 101.53 \cdot 7 + 50.77 \cdot 3.5 = 2487.56$$

BEN

It is important to keep in mind that the equivalent static force method is an approximate method, and its applicability is limited by the various assumptions and simplifications. To overcome some of the limitations and extend its applicability, the equivalent static force method is often used in conjunction with some empirical corrections or adjustments.

4.5 Earthquake Response of Inelastic Systems

In practice, designing structures to resist earthquake effects in the elastic range can be costly and inefficient. It may also be dangerous given the uncertainties involved in predicting earthquakes. The challenge in earthquake engineering is to prevent the collapse of structures with the understanding that it will deform into the inelastic range and sustain damages.

A detailed study of the nonlinear inelastic response of structures under earthquake excitation is outside the scope of this course. However, we will illustrate the key concepts using an ideal elastic-perfectly plastic (elastoplastic) system.

4.5.1 Force-Deformation Relations

Since the 1960's hundreds of laboratory tests have been conducted to characterize the behaviour of structural members and components under earthquake conditions. How a structure behaves under earthquake loading depends greatly on the material and structural system. Two examples are shown in Figure 4.18.

Dissipated E through plastic deformation

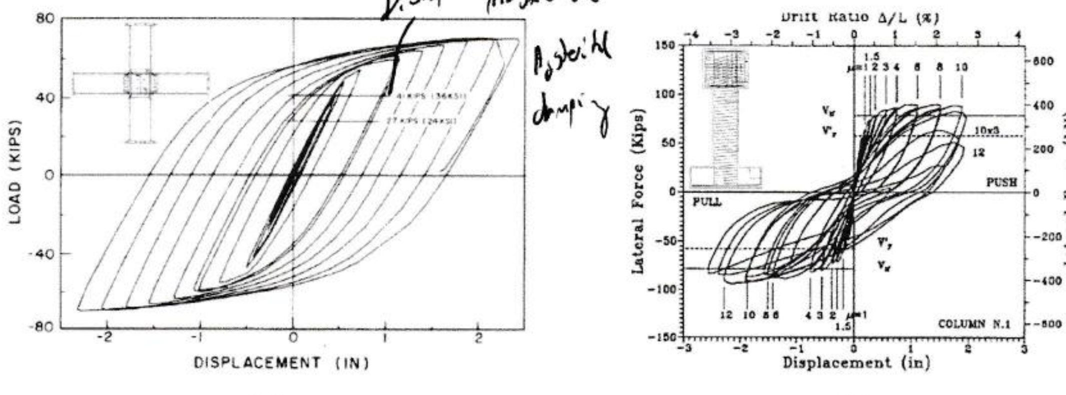

(a) **(b)**

Figure 4.18 Force-deformation behaviour under cyclic loading
(a) Structural steel[1] **(b)** Reinforced concrete[2]

The force-deformation plots in Figure 4.18 show repeated loading and unloading cycles with reversal of deformation, simulating the oscillatory motion that occurs in earthquakes. In steel structures, stiffness and strength are largely unchanged even after several cycles as long as

[1] Popov, E. P. (1987). "Panel zone flexibility in seismic moment joints," *J. Constr. Steel Res.*, 8, 91-118.
[2] Priestley, M. N., & Benzoni, G. (1996). "Seismic performance of circular columns with low longitudinal reinforcement ratios," ACI Struct. J., *93*(4), 474-485.

no

instabilities are avoided and P-delta effects are not significant. In reinforced concrete, noticeable degradation of stiffness and strength occur.

One characteristic common in the force-deformation curves shown above is the development of *hysteresis loops* as the structural component deforms into the inelastic range. Earthquake energy is dissipated when permanent deformation is left in a structure. The area under each hysteresis loop represents the dissipated energy. This energy dissipation known as *hysteretic damping*, is crucial in strong earthquakes.

As can be seen, the true behaviour of structural materials is nonlinear and complex. For our purposes, we will use the elastoplastic idealization shown below.

does not harden

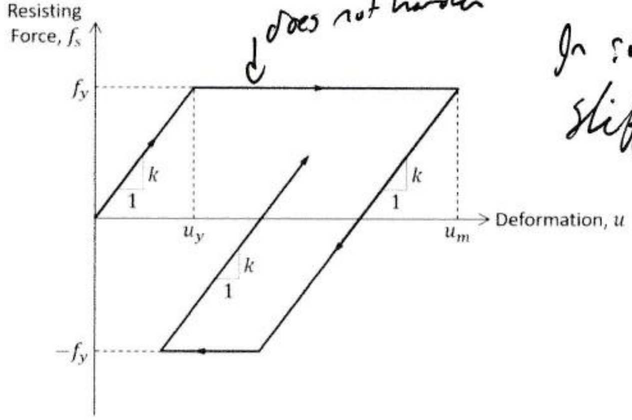

In idealized material, stiffness do degrade. False in real life

Figure 4.19 Elastoplastic force-deformation relation

u_y and f_y represent the yield deformation and yield strength respectively, and u_m is the peak deformation of the elastoplastic system. The yield strength f_y is the same in the two directions of deformation and unloading and reloading follow a path parallel to the initial elastic branch. The cyclic force-deformation relation is path dependent, meaning, for deformation u at time t, the resisting force f_s depends on the prior history of motion of the system and whether the deformation is currently increasing or decreasing. Thus, the resisting force is an implicit function of deformation (i.e. $f_s = f_s(u)$).

Let us also define a very important parameter in earthquake engineering. *Ductility*, commonly denoted using μ is the ratio

$$\mu = \frac{u_{max}}{u_{yield}} \tag{4.74}$$

μ is the ratio of the peak deformation u_m in an earthquake to the yield deformation u_y. It signifies the demand imposed on the structure in an earthquake and the amount by which the system must be able to deform inelastically without collapsing.

4.5.2 Response of Inelastic Systems

The equation of motion for a nonlinear SDOF system subjected to earthquake excitation is

$$m\ddot{u} + c\dot{u} + f_s(u) = -m\ddot{u}_g \tag{4.75}$$

As discussed briefly in Section 4.1.2, if $f_s(u)$ is nonlinear, we need additional computations in the Newmark-β algorithm to iteratively solve the dynamic equilibrium problem. There are many different numerical methods for doing this but we will skip the analysis and simply examine the response of an inelastic system. Consider the SDOF shear frame shown in Figure 4.20.

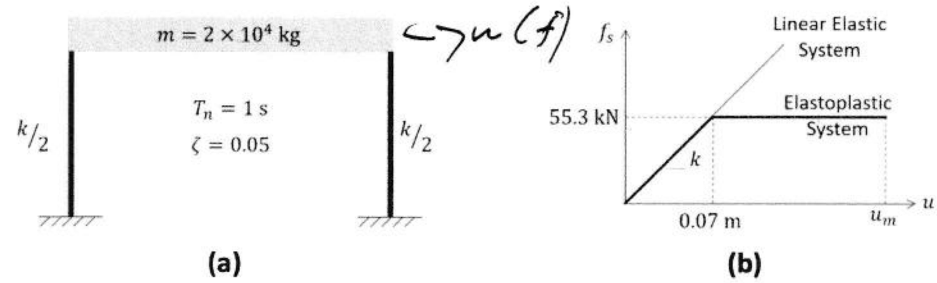

Figure 4.20 **(a)** SDOF shear frame **(b)** Force-deformation behaviour

Response to the El Centro ground motion for the linear and elastoplastic case are compared in Figure 4.22.

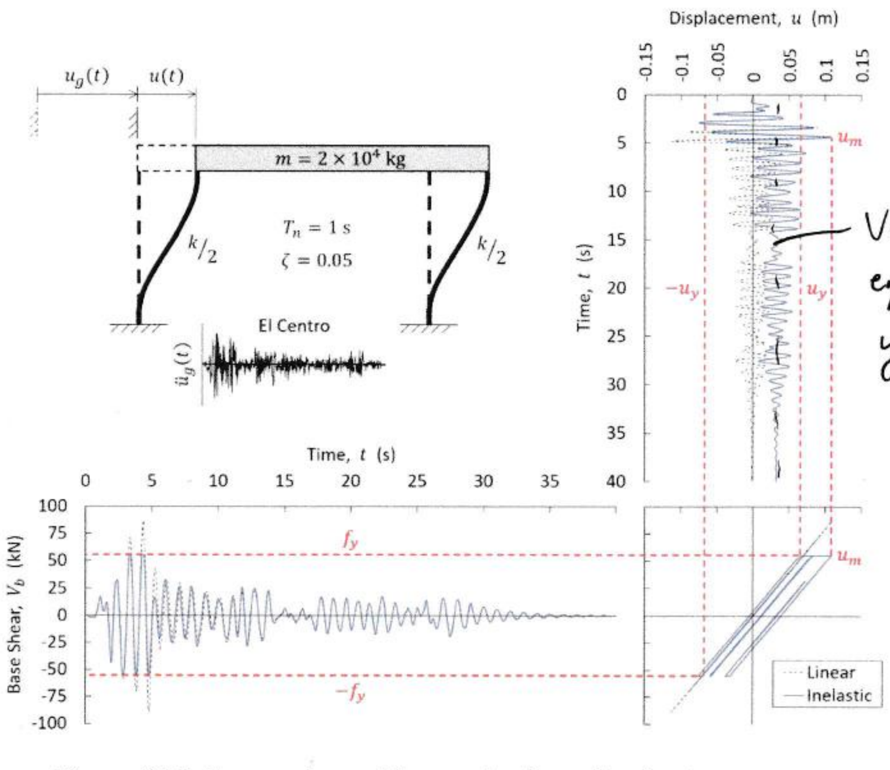

Vibrates about new equilibrium point after yielding

Figure 4.21 Comparison of linear elastic and inelastic response

- In the linear case, the peak base shear is 88.7 kN. This suggests if we can design the system with a lateral force capacity of at least 88.7 kN, it will remain elastic and withstand the El Centro ground motion with no structural damage (no plastic deformation).
- In the elastoplastic case, we can see that after yielding occurs, the system begins oscillating about a new equilibrium position. The structure sustains permanent structural damage in the form of plastic deformation.
- The peak base shear in the elastoplastic system is limited by the yield strength. This suggests we can design this system for a lower lateral force than the elastic system.
- However, to ensure the structure does not collapse, it must be provisioned with a deformation capacity that exceeds u_m.
- In other words, we can design a structure for a lower lateral force but still prevent the it from collapsing by providing adequate ductility. The cost is, of course, some structural damage. This is the key idea behind modern seismic design.

4.5.3 Energy Dissipation

When a structure is subjected to low level excitation, it can be expected to behave in a linear elastic manner and energy dissipation will occur through viscous damping. Under severe cyclic loading, structures will yield and the load-deformation behaviour will be characterized by hysteresis loops as demonstrated above in Figure 4.18.

- The area under the hysteresis loop represents energy that is dissipated as a result of the structure undergoing plastic deformations.
- This form of energy dissipation, known as *hysteretic damping*, occurs at the cost of damaging the structure and leaving permanent deformations but is crucial in large earthquakes.
- Special care is necessary when designing a structure to ensure it can undergo large deformations and numerous load reversals without significant stiffness and strength degradation.

Let us examine energy dissipation a little more closely by quantifying the effect of viscous and hysteretic damping. We can define the various components of energy in an earthquake excited inelastic structure by integrating the equation of motion as

$$\int_0^u m\ddot{u}(t)\,du + \int_0^u c\dot{u}(t)\,du + \int_0^u f_s(u)\,du \;= -\int_0^u m\ddot{u}_g(t)\,du \tag{4.76}$$

where,

$$-\int_0^u m\ddot{u}_g(t)\,du = E_I(t) = \text{Input earthquake energy}$$

E - balance

- Even though the natural period and damping ratio are identical in the linear and elastoplastic systems, the input energy is different. However, in both systems, all of the input energy is eventually dissipated.
- In the linear system, all of the input energy is dissipated by viscous damping.
- In the elastoplastic system, some of the energy is dissipated by hysteretic damping. In this particular example, the structure does not deform that far into the inelastic range so hysteretic damping does not play a huge role. In a more intense earthquake, hysteretic damping could become more significant than viscous damping.